Chapter 3. Transitions Between Electronic States - Chemical Dynamics and Kinetics

3.1 *Transitions Between States*

In this Chapter we seek a structural and pictorial representation of the photophysical transitions of Scheme 2.1 in order to develop methods for qualitatively evaluating the rate constants (k) for the radiative (*R → R + hν) and radiationless (*R → R + heat) photophysical processes that appear in the standard state energy diagram, Scheme 1.4. We shall then give exemplars of structure-reactivity and structure-efficiency relationships for n,π* and π,π* states for the processes in the state energy diagram in Chapter 4 and 5. A structural and pictorial model for the primary photochemical transitions of Scheme 2.1 (*R → I or *R → P) will be presented in Chapter 6. Indeed, photochemical reactions may be viewed as a class of radiationless transition producing a new chemical structure I or P (photochemical process) rather than the initial chemical structure R (photophysical process). Scheme 3.1 shows the transitions that will be of interest in this Chapter.

(a) $R + h\nu \rightarrow {}^*R(S_1)$; $R + h\nu \rightarrow {}^*R(T_1)$

(b) ${}^*R(S_1) \rightarrow R(S_0) + h\nu$; $R(S_1) \rightarrow R(S_0)$ + heat

(c) ${}^*R(S_1) \rightarrow {}^*R(T_1)$

(d) ${}^*R(T_1) \rightarrow R(S_0) + h\nu$; ${}^*R(T_1) \rightarrow R(S_0)$ + heat

(e) ${}^*R(T_1) \rightarrow {}^3I$; ${}^3I(D) \rightarrow {}^1I(D)$

Scheme 3.1 ***Important photophysical processes in molecular organic photochemistry: (a) Photophysical processes of light absorption from R to *R include spin allowed absorption and spin forbidden absorption; (b) Photophysical processes from $^*R(S_1)$ to R include fluorescence and internal conversion; (c) Photophysical process of intersystem crossing from $^*R(S_1)$ to $^*R(T_1)$: (d) Photophysical process from $^*R(T_1)$ include phosphorescence and intersystem crossing to R; (e) Photophysical processes from a triplet diradical (or radical pair) intermediate to produce a singlet diradical (or radical pair) intermediate.***

In Chapter 2 we were described how to construct a state energy diagram through the qualitative evaluation of the energies of the orbital configurations, vibrational wavefunctions and spin configurations, associated with a given "spatially frozen" nuclear geometry (Born-Oppenheimer approximation). This approximation allows us to focus on

energetics and *structures* which were "time independent," or so-called "average", "static", or "equilibrium" properties of isolated molecules. In this Chapter we will describe the ***transitions*** between electronic, vibrations and spin states. These transitions are considered as First Order interactions which induce transitions (1) if the electronic motion of an electron interacts with the electronic motion of another electron (***electronic interactions***); (2) if the electronic motion of an electron interacts with vibrational motion (***vibronic interactions***); of (3) if the electronic motion of an electron in a orbital interacts with it spin motion (***spin-orbit interactions***). We will use the term "mixing" of wavefunctions to describe such interactions and shall see how quantum mechanics deals with issues of mixing. We will translate the quantum mechanical interpretations of Zero Order state mixing into a qualitative, pictorial set of rules that will provide us with quantum intuition on how to think about the mixing of states.

Scheme 3.1 shows some of the important photophysical transitions following the production of *R through absorption of a photon. Examples of the radiative processes (R + hν → *R and *R → R + hν), will be discussed in Chapter 4. Examples of the radiationless processes, $R(S_1) \rightarrow R(S_0)$, $*R(S_1) \rightarrow *R(T_1)$ and $*R(T_1) \rightarrow R(S_0)$ + heat, will be discussed in Chapter 5. In Chapter 6 we shall consider primary photochemical processes, *R → I *R → F → P and *R → [*I, *P] given in the paradigm of Scheme 2.1.

Recall that through quantum mechanics, the value of any observable property of a state, Ψ_1 may be predicted by computation of an appropriate matrix element (Eq. 3.1).

$$\text{Observable Property } P_1 = \langle \Psi_1 | \mathbf{P_1} | \Psi_1 \rangle \quad \text{Matrix Element} \tag{3.1}$$

In Chapter 2 the observable properties, P_1, of interest were state properties of Ψ_1, in particular, state energies, the operator $\mathbf{P}_1$, characterized the electrical and magnetic interactions that determined the ranking of the energies of the ground electronic state, the ground vibrational state and the ground spin state and the energies of the excited states that lay above the ground states. In this Chapter we are interested in the rates of transitions between an initial state Ψ_1 (subscript 1) and a second state Ψ_2(subscript 2). If we knew the wavefunctions Ψ_1 and Ψ_2 we could predict the rate of a transition between

Ψ_1 and Ψ_2 by making a good guess at the interaction operator, $\mathbf{P}_{1\rightarrow 2}$, ***that perturbs the initial state wave function Ψ_1 and makes it "look like" the wavefunction of the final state Ψ_2.*** Knowledge of and Ψ_1, Ψ_2 and $\mathbf{P}_{1\rightarrow 2}$ allows the computation of the rate of transition between the two states by computation of a matrix element $<\Psi_1|\ \mathbf{P}_{1\rightarrow 2}\ |\Psi_2>$. The accuracy of the evaluation will depend on the level of approximation used for the wavefunctions and how good the guess is for the selection of the operator, $\mathbf{P}_{1\rightarrow 2}$, that corresponds to the interaction inducing the transition. The "Zero Order guess" of the nature of $\mathbf{P}_{1\rightarrow 2}$ is usually made by appealing to a classical mechanical model for interactions which allows the selection of the operator $\mathbf{P}_{1\rightarrow 2}$ that can induce transitions. The model is then modified to include the appropriate quantum and wave mechanical effects. Once this is done we shall express the operator and wavefunction in pictorial terms and qualitatively estimate the value of the matrix element $<\Psi_1|\ \mathbf{P}_{1\rightarrow 2}\ |\Psi_2>$. This qualitative evaluation of the matrix elements will provide useful "selection rules" for transitions shown in Sch. 3.1and will serve as a guide to their plausibility and probability for specific organic molecules. In general the first order perturbations provided by the interactions corresponding to the operator $\mathbf{P}_{1\rightarrow 2}$ will be relatively small. This will always be the case if a good Zero Order wave function has been selected for the system. The reason for this generality is that perturbations are merely refinements of the approximate Zero Order wavefunction that mix other wavefunctions into the initial wavefunction to make it "look more like" the real wavefunction.

3.2 *Chemical Dynamics as a Starting Point for Modeling Transitions between States*

According to the paradigms of chemical dynamics, all transitions between different states are impossible if any of the fundamental conservation laws (energy, momentum, charge, mass) are not obeyed. Such transitions are termed "strictly forbidden" and are considered to be impossible, ***no exceptions!*** When conservation laws are fully obeyed and changes of structure correspond to a natural extension of the "zero point" motions of the particles (orbital, vibrational, and spin motions) the transitions occur at the fastest possible rates and are limited by zero point motion and are termed

"fully allowed." Thus, the rate of any photophysical transition may range from zero (strictly forbidden) to the rate of zero point motion (fully allowed).

For the photophysical transitions shown in Sch. 3.1, we shall seek to develop "selection rules" that will provide quantum intuition to whether the rate of a process is closer to the "strictly forbidden" (implausible) or "fully allowed" (plausible) limits. The pictorial process for transitions is quite simple and is an extension of the process of visualizing states except that the notion of time dependence of a state is introduced. We start with a visualization of the wavefunctions corresponding to the initial state (Ψ_1) and final state (Ψ_2) involved in a transition $\Psi_1 \rightarrow \Psi_2$ (e.g., *R $\rightarrow$ R). With a picture of the wavefunction of the initial and final state in mind, we apply the rules of quantum mechanics to estimate the matrix element (Section 2.4) which describes the qualitative rate of the transition. The value of a property, P_1 of a single state with a wavefunction Ψ_1 may be computed from the matrix element (Eq. 3.1, compare to Eq. 2.6) if the operator $\mathbf{P}_{1 \rightarrow 2}$ which correspond to the interaction which triggers the transition is applied.

Similarly, the value of the rate of a transition between two states with wavefunctions Ψ_1 and Ψ_2 may be computed from a matrix element (Eq. 3.2) which has a similar form to Eq. 3.1.

$P_{1 \rightarrow 2} = \langle \Psi_1 | \mathbf{P}_{1 \rightarrow 2} | \Psi_2 \rangle$ Magnitude of transition rate between state 1 and state 2 (3.2)

To make a qualitative estimation of the magnitude of the matrix element of Eq 3.2, we need not only a picture of the wavefunctions (structures) of the initial and final state, but also a picture of the operator (the interactions or forces which mix the wavefunction of the initial state Ψ_1 and make it look like the wavefunction of the final state Ψ_2) and the energy differences between the initial and final states. In general, the larger the energy difference between Ψ_1 and Ψ_2 the more difficult it will be to make the states look alike, the smaller the value of the matrix element corresponding to the transition and the slower the rate of transition between the states. Thus, the physical picture behind a transition between two states is that transitions always occurs fastest when the two states are similar in energy and when the two states involved in the transition "look alike" or can be made to look alike as the result of a perturbation, $\mathbf{P}_{1 \rightarrow 2}$.

This procedure follows the principle of "minimum quantum mechanical reorganization" for the fastest transitions, where the reorganization includes molecular structure, motion and energy. By "look alike" we mean look alike in all respects. When two classical waves are similar in energy and "look very much alike" they are setup to go into resonance with one another. Quantum mechanics picks up on this classical idea and states that the wavefunctions of the two states must look alike in order for ***resonance*** to occur between the states. If the initial system (Ψ_1) goes into a state of resonance with the final state (Ψ_2). there is a certain probability that the system will wind up in the final state Ψ_2 and that a transition $\Psi_1 \rightarrow \Psi_2$ will have occurred.

3.3 Classical Chemical Dynamics: Some Preliminary Comments

We can obtain some ***classical intuition*** concerning the dynamics of molecular transitions by the ***concepts*** of classical mechanical dynamics, that obey the great conservation laws (conservation of energy and momentum), just as do quantum mechanical systems. In addition to obeying the conservation laws, the classical theory of the dynamics of mechanical systems is derived from Newton's laws and is based on two fundamental principles:

1. A central problem in understanding dynamic processes such as transitions between states is the identification of interactions (the ***forces***) involved in changing the motion of the particles in the initial state. In general these forces are electric (also termed electrostatic) or magnetic. Typically, the electrostatic forces such as electron-electron (electronic) interactions or electron-vibrational (vibronic) are much larger than the magnetic interactions (e.g., spin-orbit interactions)
2. Deviations from original dynamics result from interactions and occur reciprocally, i.e., to each action there is an equal and opposite reaction. Typically if we can identify an interaction in one direction of a transition, we can guess the nature of the interaction in the reverse direction.

The central issues in understanding transitions between states require an understanding of the changes in energy which occur as forces (interactions) change the

motions of an initial state and thereby cause transitions to occur between the initial state and another state. The interactions or forces responsible for these changes in motions correspond to the mathematical operators, $\mathbf{P}_{1\rightarrow 2}$, that are used in computing matrix elements.

The following general paradigm is fundamental to determining the mechanism of transitions between states:

> **For any transition between two states, energy and momentum may be conserved during the transition by couplings (interactions) to sources which transfer energy or momentum between the states. These sources may be internal (electronic, vibronic or spin-orbit couplings within a molecular structure) or external (energy or momentum exchanging interactions between molecules or energy or momentum exchanging interactions with radiation available from the electromagnetic field).**

The challenge in determining the mechanism of transitions between states $\Psi_1 \rightarrow \Psi_2$ is to identify the energies (energy must be conserved) and the interactions (forces must be available to change the motions of the initial system) that are possible and in a particular system and which of the possible available interactions make the transition $\Psi_1 \rightarrow \Psi_2$ plausible.

3.4 Quantum Dynamics: Transitions between States

In Chapter 2 we sought to estimate properties such relative singlet-triplet energy gaps for n,π* and π,π* states by visualization of the matrix elements for the appropriate states (Eq. 2.21a and Eq. 2.22b). In this Chapter in a similar spirit we seek to estimate the relative rates of transitions between states by visualization of matrix elements of the form of Eq. 3.2. Since we already have pictorial models for the molecular wavefunction, Ψ_0 in terms of the approximate electronic (ψ), vibrational (χ) and spin (**S**) wavefunctions, our main task will be to visualize the operators, $\mathbf{P}_{1\rightarrow 2}$, in Eq. 3.2 and how they operate on the wavefunctions to produce a final value of the matrix element.

3.5 Transitions between States: Evaluation of State Mixing and Transition Probabilities

Transitions between states are viewed quantum mechanically as being induced by interactions or forces which change the motions (of electrons, vibrations or spins) in one state and make the initial state look like the final state. These interactions or perturbations may be defined as "weak" or "strong" depending on how they distort the Zero Order wave function. As mentioned earlier, we shall mainly be concerned with weak perturbations which are responsible for triggering transitions such as those shown in Sch. 3.1. A weak perturbation, **P'**, slightly distorts the Zero Order electronic (or vibrational or spin) wave function, and this distortion can be interpreted as a "mixing" of the wave functions of the initial state Ψ_1 and the final state Ψ_2. As a result of the perturbation induced mixing, the original wave function Ψ_1 now contains a certain amount of component of Ψ_2; there is a finite probability that after the perturbation has been applied, the system will be in Ψ_2, i.e., there is a certain probability that a transition from Ψ_1 to Ψ_2 will be induced by the perturbation **P'** and the system may undergo a transition and "relax" to Ψ_2 to make the transition complete.

The modification of the approximate initial wave function Ψ_1 to make it look like the final state Ψ_2 is thus achieved by mixing into it other wavefunctions of the simple system in appropriate proportions through the interactions represented by the operator. If the correct operator (interaction) has been selected, the mixing makes Ψ_2 "look like" Ψ_1. The more the mixing makes Ψ_2 "look like" Ψ_1 the faster and more probable is the transition Ψ_1 to Ψ_2.

Quantum intuition for the mixing states is provided by ***perturbation theory***, which provides the recipe of how correctly mix states into Ψ_1 to make it look more like Ψ_2 . The general spirit of perturbation theory is to start with a simpler, solvable system of wavefunctions (e.g., Born-Oppenheimer approximation, one electron orbitals) that closely resemble the true wavefunction, as a Zero Order approximation, and then to "perturb the Zero Order wavefunction" to obtain First Order approximate wavefunctions

and energies. Using the First Order wavefunctions and energies, it is assumed that the perturbation distorts the system in the direction of the true wave function. If the simple and true wave functions are very similar, the extent of the distortion is small and a very weak perturbation can do the job. If the wavefunctions are very dissimilar, the extent of distortion required to mix the states will be large and a strong perturbation will be needed to induce the transition or the transition will be very slow. Perturbation theory provides the recipe for mixing the systems and determining the method to calculate the additional First Order terms that need to be added to make the system as close as possible to the true system.

An important general conclusion of perturbation theory is that, in general, *the larger the energy separation(ΔE) between the two states involved in the perturbation and the slower the transition, the weaker the mixing and the slower the rate of transitions and the smaller the energy separation(ΔE) between the two states involved in the perturbation, the stronger the mixing and the faster the transition*. According to perturbation theory (Eq. 3.3), the First Order correction of the Zero Order wavefunction, Ψ_0, is given by a "mixing coefficient", λ, which is directly proportional to the strength of the perturbation, **P'**, and inversely proportional to the separation of the energy between the states (ΔE) being mixed. The First Order wavefunction is obtained by multiplying Ψ_0 by λ (Eq. 3.4).

$$\lambda = (\text{strength of the perturbation } \mathbf{P'})/\Delta E \qquad (3.3)$$

$$\Psi_1\text{' (First Order Wavefunction)} = \Psi_1 + \lambda\Psi_2 \text{ (Zero Order Wavefunction)} \qquad (3.4)$$

From Eq. 3.3, we note two very important general rules of perturbation theory: (1) the stronger the perturbation, the stronger the mixing and distortion of the initial wavefunction Ψ_1 and (2) the greater the energy separation between the two interacting wavefunctions, the weaker the mixing. These simple rules indicate that for two states (Ψ_1 and Ψ_2) that are widely separated in energy relative to the perturbation, the system is generally expected to be weakly responsive to the perturbation and will not mix well (it will be relatively difficult to make Ψ_1 and Ψ_2 look alike). On the other hand, when a

transition involves two states that are very close in energy, the initial system may be very sensitive to perturbations and may be weakly perturbed even by weak perturbations (it will be easy to get Ψ_1 and Ψ_2 to look alike). When Ψ_1 and Ψ_2 get very close in energy the two systems become "easy to mix" if the correct perturbation is available to operate on the system. This ease of mixing for states that are close in energy is a characteristic ***resonance*** feature or waves. Classically, it is easier to distort a weak spring but more difficult to distort a strong spring with external perturbations. The reason for this difference lies in the energy separations of the vibrational levels of the springs, which are described by classical wavefunctions. The stiff spring has widely separated energy levels and is difficult to perturb (its wavefunctions are relatively difficult to mix) compared to a soft spring which has closely spaced energy levels and is easier to perturb (its wavefunctions are relatively easy to mix).

The rate of "fully electronically allowed" transitions is of the order of 10^{15}-10^{16} s^{-1} and is limited only by electronic motion for the transition (provided the nuclear and spin configurations remain constant). However, if the nuclear and/or spin configurations change during a "fully allowed" electronic transition, the transition may be "rate limited" by the time it takes to change the nuclear or spin configuration. In other words, the electronic part of Ψ_1 may take have a rate of 10^{15}-10^{16} s^{-1} in "looking like" Ψ_2, but the rate of the transition $\Psi_1 \rightarrow \Psi_2$ may be limited by the time it takes to make the vibrations and spins in the final state Ψ_2 look like the vibrations and spins in the initial state Ψ_1. Such a view of transitions rates provides benchmarks for the maximal rates of various "allowed" transitions. When a rate is slower than the maximal rate we can search for the structural changes in electron shape and motion, vibrational shape and motion and spin configuration and motion may serve as kinetic "bottlenecks" in determining transition rates. We may associate a "prohibition *factor*" (*f*) for each structural change (in the sense of spatial distribution or motion) involved in a transition between states. Let us define a value of $f = 1$ to mean that the transition is completely allowed and is limited only by zero point motions. If we think of the system as a harmonic oscillator (Section 2.15) "oscillating" back and forth between Ψ_1 and Ψ_2, then $f = 1$ corresponds to the fastest oscillation possible for the system, i.e., is limited by zero point motion. We say that transition Ψ_1 and Ψ_2 has an "***oscillator strength"*** of 1.

The rate constant k^0_{MAX} for the transition when $f = 1$ will be maximal. When $f < 1$, the ***observed*** rate of the transition, k_{OBS}, will be slower than the rate of zero point motion. As f decreases in value, the rate of the transition is proportionally slower. We can consider f as an indicator of the "allowedness" or the forbiddenness" of a transition. As the value of f approaches 1, the transition become "fully allowed" and as the value of f approaches 0, the transition becomes "strictly forbidden".

In dealing with molecular kinetics one is concerned with the rate constants for transitions. It is convenient to consider k_{OBS} in terms of the maximal rate constant k^0_{MAX} and the product of prohibition factors, f, for the electronic, vibrational and spin aspects of the transitions. In Eq. 3.5, for a given transition from Ψ_1 to Ψ_2, f_e is the electronic change (orbital configuration change), f_V is the prohibition factor associated with the nuclear configuration change (usually describable as a vibrational change in position or motion) and f_S is the prohibition factor associated with a spin configurational change (f_S equals 1 transitions for which there are no spin changes).

Observed rate constant	**Zero point motion limited rate constant**	**"Fully allowed" rate**
k_{OBS} =	k^o_{MAX}	x f_e x f_V x f_S (3.5)
Prohibition to maximal rate caused by "selection rules"		Prohibition factors due to changes in electronic nuclear, or spin configuration

For a radiationless transition from an initial state $\Psi_1 \rightarrow \Psi_2$, that does not involve a change in electron spin, the value of k^o_{max} is of the order of 10^{13}-10^{14} s^{-1} and is

limited by the time it takes the vibrating nuclei to execute zero point motions (Born-Oppenheimer approximation). However, the values of k_{OBS}) experimentally for photophysical processes (Chapters 4 and 5) are, in general, much smaller than 10^{13}-10^{14} s^{-1}. Thus, f_e, f_V, or f_S (or some combination) must contrive to place a prohibition on the maximum transition rate. For example, if the transition involves an orbital configuration change corresponding to a substantial change in electronic symmetry or motion along the nuclear framework, f_e may be very much less than 1.00. Similarly, if the transition involves a drastic change in nuclear configuration or motion, f_V will be very much smaller than 1.00. Finally, if the transition does not conserve total electronic spin, f_S, may be **very** much smaller than 1.00.

How do we qualitatively evaluate f_e, f_V, and f_S? For large, favorable interactions between zero order states $f_e \sim f_V \sim f_S \sim 1.00$ and $k_{obs} \sim k^o_{MAX}$. This will occur only when the initial wavefunction Ψ_1 and the final wavefunction Ψ_2 look very much alike and/or when the two wavefunctions have very similar energies. Thus if we can visualize the initial and final wavefunctions and can estimate their energies, we can decide by inspection if the transition is likely to approach the maximal rate. When this is the case, the rates and probabilities of transition close to the zero point limit and external perturbations are minimal in inducing the transition.

In most cases k_{OBS} is much smaller than k^o_{MAX}. In these cases we are concerned with *small* interactions between zero order states. The magnitude of the *f* factors (which are pure numbers), for small interactions, is approximate given by Eq. 3.6

$$f \sim [\langle\Psi_1|\mathbf{P}'_{1\rightarrow 2}|\Psi_2\rangle/\Delta E_{12}]^2 \qquad (3.6)$$

where $\langle\Psi_1|\mathbf{P}'_{1\rightarrow 2}|\Psi_2\rangle$ is the matrix element for the $\Psi_1 \rightarrow \Psi_2$ transition, and ΔE_{12} is the energy gap between the zero order states Ψ_1 and Ψ_2.

From Chapter 2 we learned how to use the Born-Oppenheimer approximation to break the true (but unattainabe) wavefunction Ψ into an approximate electronic (ψ), vibrational (χ) and spin (**S**) wavefunction. For transitions that do not involve a change in

spin ($\mathbf{S_1} = \mathbf{S_2}$), $f_S = 1$ and electronic spin does provide any prohibition on k_{OBS}. In this case *the rate of transition between Ψ_1 and Ψ_2 is either limited by the time it takes to make the electronic wavefunction ψ_1 look like ψ_2 or the time it takes for the vibrational wave function χ_1 to look like χ_2.* For organic molecules, the most important perturbation for "mixing" electronic wavefunction that initially do not look alike is vibrational nuclear motion which is coupled to the motion of the electrons. Let the operator corresponding to this coupling vibrational motion be termed $\mathbf{P}_{VIB}$ so that the matrix element for the perturbation that vibrationally mixes ψ_1 and ψ_2 is given by $\langle\psi_1|\mathbf{P}_{VIB}|\psi_2\rangle$. In general it is most important that the electronic wavefunction be distorted into a shape that will allow the transition to occur. When this is true, we need only consider the magnitude of the overlap integral of the vibrational wavefunctions, $\langle\chi_1|\chi_2\rangle$, which determines the prohibition on the transition due to **Frank-Condon factors** (to be discussed in detail in Section 3.6). From these considerations the value of k_{OBS} for a spin allowed transition will have the form given in Eq. 3.7.

$$k_{obs} = \left[\frac{k^o{}_{max} \langle\psi_1 | H_{vib} | \psi_2\rangle^2}{\Delta E_{12}{}^2} \right] x \left[\langle\chi_1|\chi_2\rangle^2 \right] \qquad (3.7)$$

Vibrational orbital coupling — **Franck-Condon factors**

When the transition $\Psi_1 \rightarrow \Psi_2$ involves a change in the spin (radiationless or radiative) the question arises as to what is the perturbation which is likely to couple states of different spin ($\mathbf{S_1} \neq \mathbf{S_2}$). In molecular organic photochemistry the most important transitions involving a change in spin are radiative or radiationless singlet-triplet or triplet-singlet transitions. For organic molecules the most important perturbation which is available to "make a pair of parallel spins look like a pair of antiparallel spins" is the coupling of the electron spin motion with the electron orbital motion (termed ***spin-orbit coupling***) which takes one of the antiparallel electron spins of a singlet state ($\uparrow\downarrow$) and "twists" it or flips it so that it makes spins parallel ($\uparrow\uparrow$). We term the operator that induced spin-orbit coupling as $\mathbf{P}_{SO}$ and the matrix element is given by $\langle\psi_1|\mathbf{P}_{SO}|\psi_2\rangle$. The latter matrix element is a measure of the strength or the energy of the spin-orbit

interactions. For simplicity, the spin wavefunctions, $\mathbf{S_1}$ and $\mathbf{S_2}$, are not considered explicitly (recall we use the symbols α and β, Table 2.1, to represent the wavefunctions of a spin up and spin down, respectively), but are assumed to be taken into account by $\mathbf{P}_{SO.}$ For transitions that involve a change in spin we can modify Eq. 3.7 to include the spin change prohibition.

$$k_{obs} = \left[\frac{k^{o}_{max} \langle \psi_1 | H_{vib} | \psi_2 \rangle^2}{\Delta E_{12}^{\,2}} \right] \times \left[\frac{\langle \psi_1 | H_{so} | \psi_2 \rangle^2}{\Delta E_{12}^{\,2}} \right] \times \left[\langle \chi_1 | \chi_2 \rangle^2 \right] \qquad (3.8)$$

Vibrational orbital coupling **Spin-orbital coupling** **Franck-Condon factors**

3.5 The Spirit of Selection Rules for Transition Probabilities

If a transition obeys the laws of conservation of energy and momentum, selection rules allow the organizations of transitions into the categories plausible and/or probable. The spirit of a *selection rule* is that within a certain set of Zero Order assumptions that assign an initial idealized geometry or symmetry for a molecular state and a set of wave functions for the electrons, nuclei, and spins (ψ, χ, **S**), the matrix element, $\langle \Psi_1 | \mathbf{P}_{1\rightarrow 2} | \Psi_2 \rangle$, corresponding to a transition probability from an initial state Ψ_1 to a final state Ψ_2 may be calculated. If the matrix element for the computed transition probability equals exactly zero, the transition is said to be "strictly forbidden" in the Zero Order approximation.

When a more realistic non-ideal symmetry or when previously ignored forces and a different operator have been included, a *new* calculation of the matrix element may yield a non-zero value for the transition rate. If this probability is still small (say less than 1% of the maximal transition probability, f much less than 1, the process is said to be plausible, but only "weakly allowed". If the matrix element computed by the new calculation for the transition is large (say close to the maximum transition rate, f is close to 1), the transition can be classified as “allowed” or probable in the sense that its rate is expected to be among the fastest of the plausible transitions. It can be seen that such qualitative descriptions can only provide a "rough" feeling for transition probabilities.

Indeed, sometimes the breakdown of selection rules is so severe that the magnitude of "forbidden" transition probability approaches that of the "allowed" transition probability. When this occurs, we have selected a poor Zero Order starting point (wavefunction, Ψ or operator **P**) of our evaluation of the transition probability.

In spite of their qualitative nature, selection rules are useful in the analysis of transitions as first approximations to determine the plausibility or the probability of a transition. To be more precise, from now on, we'll identify the term plausibility in terms of the **kinetic plausibility** that a transition will occur. Kinetics is the science which deals with the rates and rate constants, *k*, of transitions. We identify the probability of a transition as a function of the competing rates of **all** plausible transitions that can are expected from an initial state, Ψ_1. A probable process from an initial state is simply one whose rate is faster than all other processes from that state. For example, *R may undergo both photophysical and photochemical processes. If the photophysical processes have much faster than the rate of photochemical processes the photochemistry is not probable. This means at best if it occurs it will be inefficient because absorbed photons will be used mainly to return *R to R rather than convert *R to P.

Thus, the prediction of probable transitions from an initial state requires two steps: (1) the appeal to selection rules for the identification of all plausible transitions and an estimation of their rate constants, and (2) a ranking of the rate constants of all the plausible transitions with the fastest being considered the most probable and the slowest being considered the least probable. Knowledge of rate constants is crucial for an understanding of the plausibility and probability of all of the transitions in Sch. 3.1.

3.7 *Nuclear Motion; Vibronic Coupling and Vibronic States. The Effect of Nuclear Motion on Electronic Energy and Electronic Structure*

From the above discussion we deduce from Eqs. 3.7 and 3.8 that in order to understand the plausibility and probability of **spin allowed** transitions between Ψ_1 and Ψ_2 we need to devise a paradigm for evaluating the matrix elements for vibrational coupling of the electronic states of Ψ_1 and Ψ_2 (vibronic coupling). The goal is to estimate how the vibrational wavefunctions (Section 2.18) for spin allowed transitions

influence the rate of electronic transitions. The Franck-Condon factors, which we shall define shortly, are a measure of the similarity of the vibrational wavefunctions of Ψ_1 and Ψ_2. In addition to the vibrational features, if the transition involves a change of spin, we need to devise a paradigm for evaluating the matrix elements for spin-orbit coupling of Ψ_1 and Ψ_2.

Up to this point we have considered electronic states only in terms of electronic configurations for fixed nuclear geometries (Born-Oppenheimer approximation, Eq. 2.1). This approximation allowed us to generate a Zero Order description of electronic structure and electronic energy, based on an assumed fixed and **non-vibrating** nuclear geometry. Since the uncertainty principle requires that vibrational "zero point" motion occurs at all temperatures, we must consider the effect of nuclear motion on the electronic structure and electronic energy of a molecule and how this motion can induce transitions between electronic states. Our goal is to replace the "pure" classical "vibrationless" molecule with a vibrating molecule and to be able to visualize how this motion will modify our Zero Order model. We call the states of a vibrating molecule *vibronic* states rather than "pure" electronic states, because these state are constantly mixing the electronic states as the result of zero order vibrations. The basic concept is that the vibrations of a molecule distort the Zero Order electronic wave function only slightly and therefore serve as a weak perturbation on the approximate wave function, but that they will distort the approximate function so that it looks like the wavefunction of other states to which transitions may occur. This process of distortion of a wavefunction is equivalent to the mixing of the initial state with other possible (if energy and momentum are conserved) final states. If the inclusion of nuclear motion causes only a small change in the electronic energy of our Zero Order model, then we can use perturbation theory to evaluate the First Order correction and compute a more accurate vibronic energy, E_v, of the Zero Order *electronic* states. The value of E_v, according to perturbation theory is given by Eq. 3.9,

$$E_V = <\Psi_1/H_V/\Psi_2>^2/\Delta E_{12} \qquad (3.9)$$

where Ψ_1 and Ψ_2 are two "pure" Zero Order electronic states that are "mixed" or "split" by the motion of nuclei, H_V is the Hamiltonian operator that describes how the electronic energy depends on nuclear motion, and ΔE_{12} is the energy difference between the Zero Order states that are being mixed by the vibronic interaction. Eq. 3.9 is a key expression to obtain quantum intuition for transitions; it emphasizes the importance of the matrix element (note it appears as the square in Eq. 3.9) and the inverse dependence on the energy gap between the Zero Order states which are being mixed.

At this point we need some benchmarks for the values of the energy separation. What do we mean by a small or large value of ΔE_{12}? We know from perturbation theory (Eqs 3.3 and. 3.4) that if ΔE_{12} is "large" the mixing of the states will be "small" and if ΔE_{12} is "small" the mixing of the two states will be large. Intuitively, what we mean by small or large is how the mixing energy E_V compares to the energy separation ΔE_{12} of the states that are mixing. If the mixing energy E_V is small compared to the energy separation, the mixing of the state is expected to be small. In general, the value of E_V is or the order of vibrational energies (Section 2.19), which range from ca 10 kcal/mole for X-H stretching vibrations to ca 1 kcal/mol for C-C-C bending vibrations. Vibronic interactions do not change significantly for electronic states whose energy separation ΔE_{12} is, say, 50 kcal/mole. This is the situation for most ground states of organic molecules and is the reason that the Born-Oppenheimer approximation works so well for ground state molecules, i.e., vibrations in the ground state do not mix electronically excited states very effectively because the electronic energy gap between S_0 and the excited states are much larger than the vibrational energies. However, vibronic interactions are much more likely to be significant in mixing Zero Order electronically *excited* states since excited states are typically packed together with small energy gaps so that ΔE_{12} is often of the order of several kcal/mole or less. *In such cases, the electronic energy and electronic structure may vary considerably during a vibration* and vibrational motion can be very effective in a mixing state. Such effects are of great importance in triggering and therefore determining the rates of transitions from excited states.

As a simple example of the effect of vibrational motion on the electronic orbital and electronic energy, consider the effect of vibrations of a carbon atom that is bound to

three other atoms (e.g., a methyl group as a radical, anion, or carbonium ion). When the system is planar and the angles between the atoms are 120^{o}, the "pure" *p* orbital may be described as a "free valence" orbital. What happens to the shape and energy of this orbital as the molecule vibrates? If the vibrations do not destroy the planar geometry (angles between the atoms change but system remains planar), the spatial distribution of the free valence orbital above and below the plane must be *identical* because of the symmetry plane (Fig. 3.1, upper). In other words, if we put electrons into the free valence orbital, the electron density would have to be the same above and below the symmetry plane, since all conceivable interactions on one side of the plane are identical to those on the other side. In effect, *the p orbital remains essentially "pure p" during the in plane planar bending vibration and the energy of the orbital is not expected to change significantly*. We say that weak vibronic coupling of electronic and vibrational motions occurs during this vibration and the distortion of the p wavefunction induced by vibrations is small.

Now consider a bending ("umbrella flipping") vibration which *breaks* the planar symmetry of the molecule (Fig. 3.1 lower). Intuitively we expect the "pure *p*" orbital to change its shape in response to the fact that more electron density (due to the bonds) are on one side of the plane. We say that a *rehybridization* of the carbon atom occurs and one can imagine that the "pure *p*" orbital begins to take on s-character, i.e., *the out of plane vibration converts the p orbital into a* sp^{n} *orbital*, where *n* is a measure of the "*p* character" remaining. Since an s-orbital is considerably lower in energy than a p-orbital, the mixing due to vibrational motion can change the energy of the orbital significantly. In the extreme situation n = 3, we imagine that the out-of-plane vibration causes a continual oscillating *p* (planar) ↔ *sp*3 (pyramidal) electronic change. We say that a significant vibronic coupling of electronic and nuclear motion occurs due to this vibration, causing the value of n to oscillate between 2 and 3. Now if the initial state, Ψ_1, is a pure p wavefunction and the final state, Ψ_2, is a pure sp^3 state, we can see that the out of plane vibrational motion makes Ψ_1 "look like" Ψ_2, but the in plane vibrational motion does not because the in plane bending vibration does not introduce any s character to the unoccupied orbital. The out of plane vibrational motion "mixes" "free valence" orbital

may be described as $_2$, but the in-plane vibrational motion does not. In a convenient short hand we can write $\Psi_1(p, \text{planar}) \leftrightarrow \Psi_2(sp3, \text{pyramidal})$

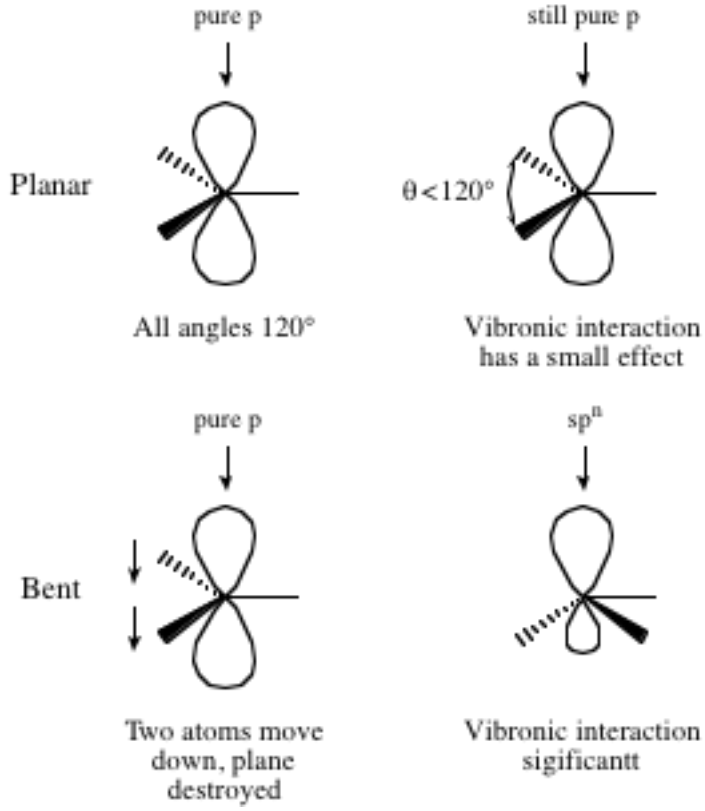

Figure 3.1. ***The effect of vibronic motion on the hybridization of a p orbital.***

In summary, we have deduced that some, but not all, vibrations are capable of perturbing the wavefunctions and the electronic energy of Zero Order electronic states. The energy difference of the Zero Order electronic levels and vibronic levels may be small relative to the total electronic energy, yet the matrix element $\langle\Psi_1/H_V/\Psi_2\rangle$ may "provide a mechanism" for transition from one vibronic state to another, even though the transition is strictly forbidden ($\langle\Psi_1 \mid \mathbf{H}_V \mid \Psi_2\rangle = 0$) in the Zero Order approximation. From a classical viewpoint, momentum is conserved by coupling electronic motion with vibrational motion. In the example discussed above, the "pure *p*" orbital did *not* undergo a momentum change during the in-plane vibration, but the non-planar vibration allowed a change in nuclear motion to be accompanied by an exchange of momentum between nuclear and electronic motion. An electron in a "pure *p*" orbital has different orbital

angular momentum from an electron in a sp3 orbital, so that conservation of total momentum is achievable by coupling the planar/non-planar nuclear momentum with the p ↔ sp3 orbital momentum change.

3.8 *The Effect of Nuclear Vibrations on Transitions between States; The Franck-Condon Principle*

We now consider the effect of nuclear vibrations on the rates of electronic transitions. Which is more likely to be rate determining for an electron transition between two states of the same spin, the electronic motion or the nuclear motion? The basis of the Born-Oppenheimer approximation (Section 2.2) is that electron motion is so much faster than and nuclear motion that the electrons "instantly" adjust to any change in the position of the nuclei in space. Since an electron jump between orbitals (Chapter 1, Section 1.13) generally takes of the order of 10^{-15}-10^{-16} s to occur, whereas nuclear vibrations takes of the order of 10^{-13}-10^{-14} s to occur, we see that the electron jump is usually faster and will not be rate determining, for transitions between electronic states $\Psi_1 \rightarrow \Psi_2$. Thus, the transition rate between electronic states (of the same spin) is limited by the ability of the system to adjust to the nuclear configuration and motion after the change in the electronic distribution. Our quantum intuition tells us that we should expect that the rate of transitions induced by vibrations (nuclear motion) will depend not only on how much the electronic distributions of the initial and final state "look alike" and also how much the nuclear configuration and motion in the initial and final states "look alike". The Franck-Condon principle, which takes the "look alike" requirements of vibrational features in Ψ_1 and Ψ_2 into account, is the paradigm governing the rates and probabilities of radiationless and radiative transitions between the vibrational levels of different electronic states (when there is no spin change occurring in the transition). When there are spin changes during the transition, spin-orbit contributions have to be taken into account.

In classical terms, the Franck-Condon principle states that ***because nuclei are much more massive than electrons (mass of a proton = ca. 1000 times the mass of an electron), an electronic transition from one orbital to another takes place while the***

massive, higher inertial nuclei are essentially stationary. This means that, at the instant that a radiationless or radiative transition takes place between Ψ_1 and Ψ_2 (e.g., between a $S_2(\pi,\pi^*)$ state and a $S_1(\pi,\pi^*)$ state) the nuclear geometry momentary remains fixed while the new electron configuration readjust themselves from the old nuclear geometry. In classical terms, electrons, being light particles, have difficulty transferring their angular momentum (due to orbital motion) into the momentum of the heavier nuclei, i.e., the conversion of electronic energy into vibrational energy is likely to be the rate determining step in an electronic transition between states of different nuclear geometry (but of the same spin).

Expressed in quantum mechanical terms, the Franck-Condon principle states that ***the most probable transitions between electronic states occur when the wavefunction of the initial vibrational state (χ_1) most closely resembles the wavefunction of the final vibrational state (χ_2).*** In analogy to the orbital overlap integral (Eq. 2.19), which defines the extent of overlap of a pair of electronic wavefunctions, we can define vibrational overlap integral in terms of the extent of a pair of vibrational wavefunctions, χ_1 and χ_2. and use the symbol $<\chi_1|\chi_2>$ to indicate the overlap integral of the two vibrational wavefunctions χ_1 and χ_2. Since in general two wavefunctions have the greatest resemblance (look most alike) when the vibrational overlap integral $<\chi_1|\chi_2>$ is closer to 1, the larger the value of the integral the more probable is the vibronic transition.

In the following sections we shall see that the Franck-Condon principle provides a useful visualization of both radiative and radiationless electronic transitions as follows: (a) for radiative transitions, nuclei *motions and geometries* do not change during the time it takes for a photon to "interact with", to be "absorbed," and cause an electron to jump from one orbital to another; and (b) for radiationless transitions, nuclear *motions and geometries* do not change during the time it takes an electron to jump from one orbital to another.

3.9 *A Classical and Semiclassical Model of the Franck-Condon Principle and Radiative Transitions*

In the classical harmonic oscillator approximation (Section 2.15), the energy of the vibrations of diatomic molecules were discussed in terms of a parabola in which the potential energy (PE) of the system was displayed as a function of the displacement, Δr_e, from the equilibrium separation of the atoms (Eq. 2.24, Figures 2.3 and 2.4). The harmonic oscillator approximation applies to both ground states (R) and excited states (*R) and to both radiationless and radiative photophysical transitions. Let us consider how the Franck-Condon principle and Franck-Condon factors apply to a radiative transition between two states in terms of the harmonic oscillator model. Figure 3.2 shows classical PE curves for a diatomic molecule that behaves as a harmonic oscillator. The top half of Fig. 3.2 is a representation of a classical harmonic oscillator for which one of the vibrating masses is very large and the other is a much lighter mass. Three PE curves (Figure 3.2, a, b, and c) are shown for three situations with respect to the initial relative nuclear geometries of a ground state (R) and an excited state (*R): (a) the equilibrium nuclear separation, r_{XY}^* of the ground state (R) is essentially identical to the equilibrium nuclear separation, r_{XY}^*, of the electronically excited molecule, (*R); (b) the equilibrium nuclear separation, r_{XY}, of (R) is slightly different from the equilibrium nuclear separation, r_{XY}^* of the electronically excited molecule, (*R), with the latter being slightly longer because of (an assumed) slightly weaker bonding resulting from electronic excitation; (c) the equilibrium nuclear separation, r_{XY}, of (R) is considerably different from the equilibrium nuclear separation, r_{XY}^*, of the electronically excited molecule, (*R), with the latter being slightly longer because of the (assumed) much weaker bonding resulting from electronic excitation. The difference in excess vibrational energy, ΔE_{vib}, is larger the larger the difference ($\Delta r = |r_{XY}^* - r_{XY}|$) in the equilibrium separations of R and *R: zero for case (a), small for case (b) and large for case (c).

Under each curve we represent the classical vibrating diatomic molecule as a vibrating ball attached to a spring, which is affixed to a wall. This would be analogous to a light atom (ball) that is bonded to a much heavier atom (the wall), i.e., a CH vibration. Most of the motion of the two atoms is due to the movement in space of the lighter particle, the H atom.

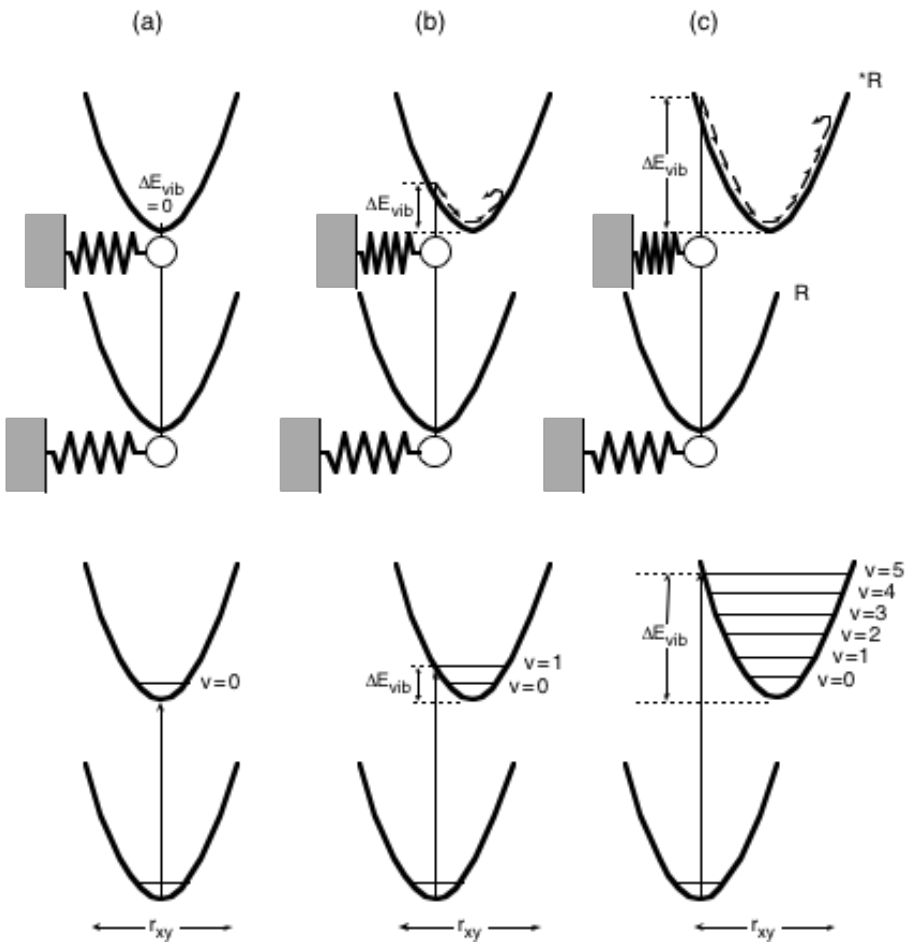

Figure 3.2. ***A mechanical representation of the Franck-Condon principle for radiative transitions. The motion of a point representing the vibrational motion of two atoms is shown by a sequence of arrows along the potential energy curve for the vibration in the top set of curves. See text for discussion.***

Now let consider a radiative HOMO → LUMO orbital transition from R to *R. which typically occurs on a time scale of 10^{-15}-10^{-16} s. According to the Franck-Condon principle, the nuclear geometry (separation of the two atoms) does not change during the time scale of an electronic transition or orbital jump, i.e., at the instant of electronic transition the internuclear separation, $r_{XY} = r_{XY}^{*}$. Thus, the geometry produced on the upper surface by a radiative transition from a ground state R to an electronically excited state *R is governed by the relative positions of the potential energy surfaces controlling the vibrational motion of R and *R. If, for simplicity, we assume that the PE curves have similar shapes, and that one the minimum of one curve lies directly over the other (Fig.

3.2a), the Franck-Condon principle states that the most probable radiative electronic transitions would be from an initial state that has a separation of r_{XY} in R which is the same as the separation, r_{XY}, of the excited state *R. Since the two curves are assumed to lie exactly over one another, the most favored Franck-Condon transition will occur from the minimum of the ground surface to the minimum of the excited surface, i.e., electronic transition from R would occur without producing vibrational excitation in *R.

In general, we may regard radiative transitions as occurring from the *most probable* nuclear configuration of the ground state, R, which is the static, equilibrium arrangement of the nuclei in the classical model and is characterized by a separation $r_{XY}^{Eq.}$ When the radiative electronic transition occurs, the nuclei are "frozen" during the transition (which is an electronic transition and occurs so fast that the massive nuclei cannot move significantly during the time scale of transition). For concreteness, let us consider the absorption of light from the HOMO of formaldehye (a n_O orbital) to its LUMO (a π^* orbital). At the instant of completion of the electronic transition the nuclei are still in the same equilibrium geometry that they were before the transition because the electronic jump occurs much faster than the nuclear vibrations. However, as the result of the orbital transition the electron density of *R about the nuclei is different from the electron density of R about the nuclei. In Figure 3.2a, since the equilibrium separation of R and *R are identical, this corresponds to a situation for which the electron distribution in $R(n,\pi*)$ is very similar to that of $R(n_O^2)$. On the other hand, the situations for Figure 3.2b and Figure 3.2c are representative of a slightly (b) and considerably (c) difference in the electronic distribution of R and *R and an accompanying difference in the equilibrium separation of the two states. These situation might correspond to a $\pi \rightarrow \pi*$ transition or to a $n \rightarrow \sigma^*$ transition.

In case (a) since the initial and final geometries of R and *R are assumed to be identical, there is no significant change in vibrational properties resulting from electronic excitation from R to *R. However, in cases (b) and (c), the electronic transition initially produces a *vibrationally excited and an electronically excited species* as the result of the new force field experience by the originally stationary nuclei of R. The atoms in *R will suddenly burst into a new vibrational motion in response to the new force field of *R. In the case of the n,π^* state, an electron has been promoted into a π^* orbital which will tend

to make the C-O bond stretch and become longer. This new force, provided by the sudden perturbation of the creation of a π* electron will induce a vibration along the C-O bond. The new vibrational motion of the molecule in *R(n,π*) may be described in terms of a *representative point*, which represents the value of the internuclear separation and which is constrained to follow the potential energy curve and execute harmonic oscillation. The vibrational motion is indicated by the arrows on the potential energy surface. The maximum velocity of the motion of the point depends on the excess vibrational kinetic energy which was produced upon electronic excitation.

For the classical case of Figure 3.2 b and c, *it follows that the original nuclear geometry of the ground state is a turning point of the new vibrational motion in the excited state, and that vibrational energy is stored by the molecule in the excited state*. A line drawn vertically from the initial ground state intersects the upper potential-energy curve at the point which will be the turning point in the excited state. For this reason, radiative transitions are termed *vertical* transitions with respect to nuclear geometry since the nuclear geometry (r_{XY} horizontal axis) is fixed during the transition. The length of the line (vertical axis) corresponds to the energy that is absorbed in the transition, i.e., the energy of the absorbed photon. Since the total energy of a harmonic oscillation is constant in the absence of friction, any potential energy that is lost as the spring decompresses, is turned into kinetic energy of the two masses attached to the spring, which is used to recompress the spring. Therefore, the potential energy at the turning points, E_{vib}, determines the energy at all displacements for that mode of oscillation.

Let us now consider a "semiclassical" model in which the effect of quantization of the harmonic oscillator and zero point motion on the classical model for a radiative electronic transition is considered (we'll consider the wave character of vibrations in the next section). In Chapter 2 (Section 2.16) we learned that the effect of quantization of the harmonic oscillator results in the restriction that only certain vibrational energies are allowed. As a result the classical PE curves must be replaced by PE curves displaying the quantized vibrational levels (bottom half of Figure 3.2). For example, Figure 3.2a (bottom) shows the ground state potential energy curve with a horizontal level corresponding to the v = 0 vibrational level. This level corresponds to a small range of geometries, determined by zero vibrational point motion, with the classical equilibrium

geometry as the center. Radiative transitions will, therefore, initiate from this small range of geometries. In case 3.2 a (bottom) the most probable transition is from the v= 0 of R to the v = 0 level of *R. In case 3.2 b the most probable transition is from the v= 0 of R to the v = 1 level of *R. In case 3.2 c the most probable transition is from the v= 0 of R to the v = 5 level of *R. As we go from case (a) to case (b) to case (c), the amount of vibration excitation produced in *R by the electronic transition increases.

The final step in our consideration of the Franck-Condon principle and radiative transitions is to visualize the wave functions corresponding to the vibrational levels of R and *R and see how their mathematical form controls the probability of electronic transitions between different vibrational levels and leads to the same conclusion as the classical case for vibrational transition.

3.10 The Franck-Condon Principle and Radiative Transitions

As we have discussed in Chapter 2 (Section 2.18), in quantum mechanics the classical concept of the precise position of nuclei in space and associated vibrational motion is replaced by the concept of a *vibrational wave function*, χ, which "codes" the nuclear configuration and momentum, but is not as restrictive in confining the nuclear configurations to the regions of space bound by the classical potential-energy curves of a harmonic oscillator. In classical mechanics the Franck-Condon principle states that the most probable electronic transitions are those possessing a similar nuclear configuration and momentum in the initial and final states at the instant of transition. In quantum mechanics the Franck-Condon principle is modified to state that the most probably electronic transitions are those which possess vibrational wavefunctions that “look alike” in the initial and final states at the instant of transition. A net mathematical positive overlap of vibrational wave functions means that the initial and final states possess similar nuclear configurations and momentum. The magnitude of this overlap is given by the *Franck-Condon integral* $\langle\chi_1|\chi_2\rangle$, in which the subscripts 1 and 2 refer to initial and final states, respectively. The probability of any electronic transition is directly related to *the square* of the vibrational overlap integral, i.e., $\langle\chi_1|\chi_2\rangle^2$, which is called the ***Franck-Condon factor.*** The larger the Franck-Condon factor, the greater the net constructive

overlap of the vibrational wavefunctions and the more probable the transition. Thus, an understanding of the factors controlling the magnitude of $<\chi_1|\chi_2>^2$ is crucial for an understanding of the probabilities of radiative and radiationless transitions between electronic states. The Franck-Condon factor may be considered as a sort of nuclear "reorganization energy", similar to entropy, that is required for an electronic transition to occur. Recall that high organization implies a small amount of entropy and a small amount of organization implies a large degree of entropy. The greater the reorganization energy the smaller the Franck-Condon factor and the slower the electronic transition. The larger the Franck-Condon factor, the smaller the reorganization energy and the more probable the electronic transition.

The Franck-Condon principle provides a selection rule for the *relative probability of vibronic transition* and the rule is applied to the *relative probability of vibronic transitions*. Quantitatively, for radiative transitions of absorption or emission the Franck-Condon factor $<\chi_1|\chi_2>^2$ *governs* the relative intensities of vibrational bands in electronic absorption and emission spectra. We shall see that in radiationless transitions the Franck-Condon factor is also important in the determination of the rates of transitions between electronic states. Since the value of $<\chi_1|\chi_2>^2$ parallels that of $<\chi_1|\chi_2>$, we need only consider the Franck-Condon integral itself, rather than its square, in qualitative discussions of transition probabilities. We obtain considerable "quantum intuition" by noting that the larger the difference in the vibrational quantum numbers for χ_1 compared to χ_2, the more likely it is that the equilibrium shape and/or momentum of the initial and the final states are different, and the more difficult and slower and less probable will be the transition $\chi_1 \rightarrow \chi_2$. Indeed, this is exactly the result anticipated from the classical Franck-Condon principle. In other words, the product $<\chi_1|\chi_2>$ is related to the probability that an initial state χ_1 will have the same equilibrium shape and momentum as χ_2.

The Franck-Condon overlap integral is mathematically and quantum mechanically analogous to an electronic overlap integral $<\psi_1|\psi_2>$, i.e., poor overlap means the two wavefunctions do not look very much alike and, as a result, corresponds to weak interactions between the wavefunctions, poor resonance, slow transition rates and a low probability of transition in competition with other plausible transitions form the given

state. Of course, the same kinds of quantum intuition can be extended to spins. In this case we are generally only concerned with two types of wavefunctions for *R, singlets and triplets. We have seen from the vector model discussed in Section 2.26 that these two types of wavefunctions do not look alike at all! They require spin-orbit coupling to distort an initial spin state to make it look like a different spin state and thereby induce intersystem crossing.

As an example of how the Franck-Condon factor controls the probability of radiative transitions, consider Figure 3.3, a schematic representation of the quantum mechanical basis of the Franck-Condon principle for a radiative transition from an initial ground electronic state ψ_1 (i.e., R) to a final electronic excited state $^*\psi_2$ (i.e., *R). Absorption of a photon is assumed to start from the lowest energy v = 0 level of ψ_1. The most likely radiative transition from v = 0 of ψ_1 to a vibrational level of $^*\psi_2$ will correspond to a vertical transition for which the overlap integral for χ_1 and $^*\chi_2$ is maximal. As shown in Fig. 3.3, this corresponds to the v = 0 $\rightarrow$ v = 4 transition. Other transitions from v = 0 to vibrational levels of ψ_2^* (e.g., from v = 0 if ψ_1 to v = 3 and v= 5 of $^*\psi_2$) may occur, but with lower probability because of the smaller overlap of χ_1 and $^*\chi_2$ for these transitions. A possible resulting absorption spectrum is shown above the potential energy curves for ψ_1 and $^*\psi_2$.

The same general ideas of the Franck-Condon principle will apply to emission, except the important overlap is then between χ_0 of $*\psi_2$ (the equilibrium position of the excited state) and the various vibrational levels of ψ_1. Experimental examples of the Franck-Condon principle in radiative transitions will be discussed in Chapter 4.

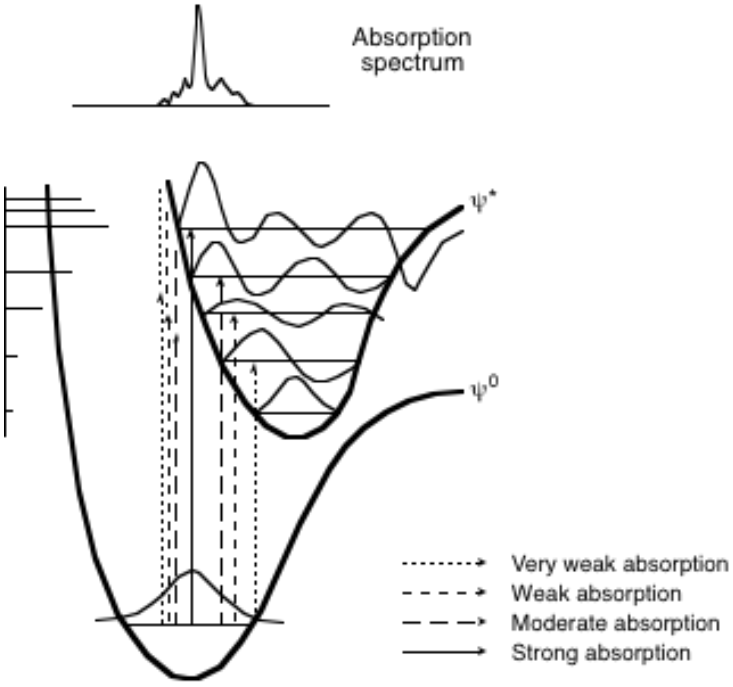

Figure 3.3. ***Representation of the quantum mechanical Franck-Condon interpretation of absorption of light. (adapted from)***

3.11 *The Franck-Condon Principle and Radiationless Transitions*

The Franck-Condon principle states that there will be a preference for "***vertical***" jumps between potential energy curves for the representative point of a molecular system during a **radiative** transition. The classical and quantum mechanical ideas behind the Franck-Condon principle can be extended to radiationless transitions. In contrast, the same Franck-Condon principle for radiationless transitions **prohibits vertical jumps in radiationless processes** (between curves separated by large energy gaps) but favors jumps at point for which curves cross or come close together. The idea is the same for radiative or radiationless transitions: a small change in the r coordinate is favored and energy must be conserved during the transition. The connection between the quantum mechanical interpretation of radiationless transitions in terms of the Franck-Condon factor, $\langle\chi_1|\chi_2\rangle$, and the motion of the representative point of a potential-energy surface may now be made.

We'll now consider the Franck-Condon principle from another point of view in Fig. 3.4. Suppose a molecule starts off on an excited PE curve corresponding to the electronically excited state whose wavefunction is $\psi_2(^*R)$. The representative point, during its zero-point motion, makes a relatively small amplitude oscillating trajectory between points A and B on the excited surface. For a transition from the $\psi_2(^*R)$ curve to the ground state curve $\psi_1(R)$ to be *possible*, energy and momentum must be conserved. Classically, a "jump" to the lower surface $\psi_1(R)$ which conserves energy, will require either an abrupt change in geometry (i.e., a ***horizontal*** "jump" from B → D (or A →C) for which the total potential energy remains constant, Fig. 3.4, left) or an abrupt transformation of potential energy to a very large amplitude oscillation (i.e., a ***vertical*** "jump" from A → E (or B → F) which sets the system into a violent oscillation between points C and D). The net result of either jump is that the vibration of the molecule will abruptly change from a placid, low-energy vibration between points A and B to a violent, high-energy vibration between points C and D. In these transitions, the positional and momentum characteristics of the vibration change drastically and such transitions are resisted classically. Let us see how quantum mechanics handles this situation mathematically.

. From the quantum point of view, the vibrational wavefunctions for the initial state (χ_i) and the final state (χ_f) of the two energy curves of Fig. 3.4 do not look at all alike. The mathematical form of the vibrational wavefunctions χ_i and χ_f for the initial and final vibrations are shown in Figure 3.5 for a radiationless transition similar to that of Fig. 3.4 (surfaces far apart for all values of r, Fig. 3.5, left) and for a radiationless transition for which the two surfaces come close together (and "cross" for some value of r). Recall that for a radiative or radiationless transition to be probable according to the Franck-Condon principle, there must be net positive overlap between these wavefunctions.

By inspection of the curves in Fig. 3.5, for the case for which the two surfaces involved in the radiationless transition are far apart for all values of r (Fig. 3.5, left), the vibrational wave function χ_i (positive everywhere, no node) associated with $^*\psi_2$ (plotted above the classical curve representing the excited state $^*\psi_2$) is drastically different in form from the vibrational wavefunction χ_f (highly oscillatory between positive and

negative values) associated with ψ_1 (plotted above the classical curve representing ψ_1) at the energy at which the transition occurs. If we imagine the mathematical overlap integral of χ_i and χ_f (the overlap integral $< \chi_i | \chi_f >$), the net overlap will be zero or close to zero because the initial function (χ_i) is positive everywhere about the point $r_{eq,}$ (the equilibrium separation), but the final function (χ_f) oscillates many times between positive and negative values about $r_{Eq.}$ The result is an effective cancellation of the mathematical overlap integral. The quantum intuition tells us, as does the Franck-Condon principle, that if the overlap integral $< \chi_i | \chi_f >$ is very small, the probability of the radiationless transition from ψ_I to ψ_f will be very small. Simply stated, the wavefunctions χ_I and χ_f "do not look very much alike" and are difficult to make look alike through electronic couplings. In terms of a selection rule, a transition as shown in Figure 3.4 in considered to be possible but to occur at a slow rate.

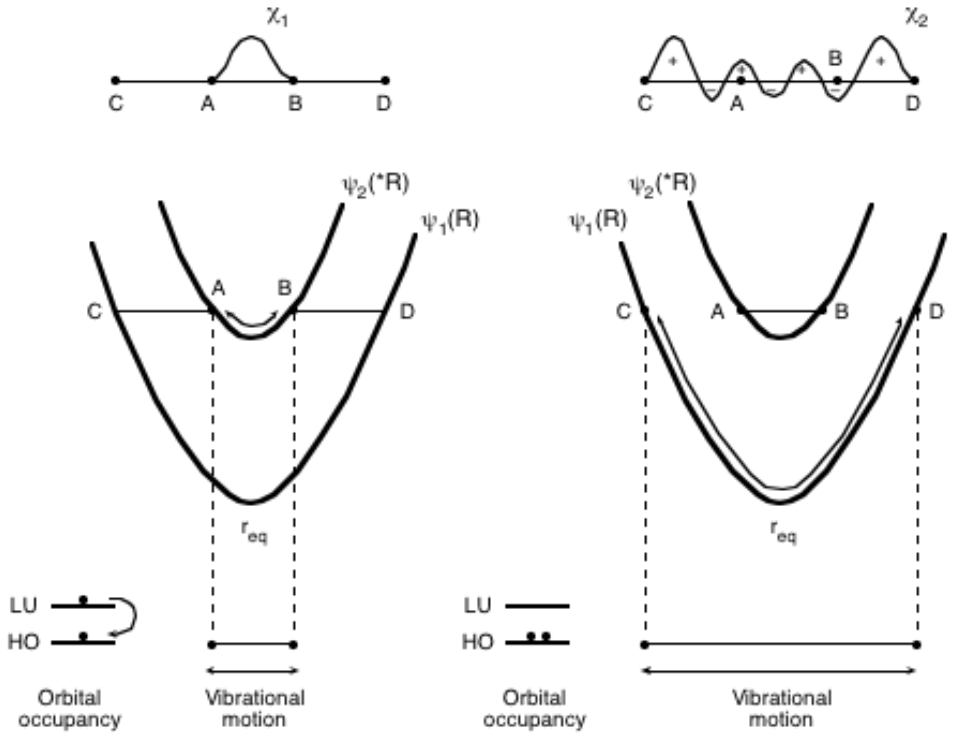

Figure 3.4. ***Visualization of the quantum mechanical basis for a slow rate of radiationless transitions due to low positive overlap of the vibrational wavefunctions.***

A vertical jump from $*\psi_2 \rightarrow \psi_1$ may be thought of as one for which a rate-limiting electron perturbation occurs first and promotes the transition from $*\psi_2 \rightarrow \psi_1$. Nuclear motion is now suddenly controlled by the $\psi_1$surface rather than $*\psi_2$, and coupled molecular acceptor vibrations of ψ_1 (or the intermolecular collisional energy acceptors in the environment) must now be found to absorb the excess potential energy associated with the jump. The horizontal jump may also be regarded as one for which a rate-limiting nuclear geometry perturbation occurs first and promotes the electronic transition from $*\psi_2 \rightarrow \psi_1$ through the geometry jumps A→ C (or B → D). Electronic motion then suddenly switches from that of $*\psi_2$ to that of ψ_1. The vibration that brings$\varpi$from A → C (or B → D) may also act as an acceptor of the excess energy. The horizontal jump is related to quantum mechanical "tunneling", and can be interpreted as being due to the very small overlap χ_i and χ_f outside the regions of the classical potential-energy curves. Thus, we conclude that radiationless transitions for which the ground state and excited state curves occur in regions of space for which there is no intersection of the two curves are always expected to be relatively slow, and from perturbation theory (Eq. 3.9) to get slower as the gap between the energy of $*\psi_2$ and ψ. increases.

In Fig. 3.5, right at a specific value of r, *curve crossing* occurs between the wavefunctions ψ_1 and $*\psi_2$. Now let us see how visualization of the overlap of vibrational wavefunctions can provide some insight to the operation of the Franck-Condon Principle. The poor overlap of the vibrational wave functions χ_i and χ_f for a molecule in the lowest vibrational level of $*\psi_2$ for the non-crossing situation (Figure 3.5 left) contrasts with the significant overlap for the curve crossing situation (Figure 3.5, right). In both cases, χ_i corresponds to the v = 0 level of $*\psi_2$, and χ_f corresponds to the v = 6 level (6 nodes in the wavefunction) of ψ_1. The amount of electronic energy ΔE_{el} that must be converted into vibration energy and the vibrational quantum number (v) of the state produced by the transition are the same for both transitions shown in Fig. 3.5. The vibrational overlap integrals $< \chi_i | \chi_f >$ for the crossing and non-crossing situations are shown at the bottom of Figure 3.5. Thus, in agreement with the classical Franck-Condon principle, quantum intuition clearly states that radiationless transition for the surface crossing situation on the right of Figure 3.5 will occur much faster than the non-surface crossing radiationless

transition on the left of Figure 3.5, because the vibrational overlap integral $< \chi_i | \chi_f >$ is clearly larger for the situation on the right. In terms of a selection rule, we say that a radiationless transition at a surface non-crossing geometry on the left is *Franck-Condon forbidden* (i.e., the Franck-Condon factor $<\chi_i|\chi_j>$ is ~ 0), whereas a radiationless transition at the surface crossing radiationless transition on the right is *Franck-Condon allowed* (i.e.,the Franck-Condon factor $<\chi_i\chi_j> \neq 0$).

We conclude that, with respect to the Franck-Condon factors, a radiationless transition from $*\psi_2 \rightarrow \psi_1$ will be very slow for the disposition of curves shown on the left of Figure 3.5 relative to the disposition of the curves on the right of Figure 3.5. We are in position to make a general statement concerning the relative rates of radiationless transitions from *R to R for any organic molecule. ***Radiationless transitions are most probable when two curves cross (or come close to one another), because when this happens it is easiest to conserve energy, motion and phase of the nuclei during the transition in the region of the crossing***.

It should be pointed out that it has been assumed that the vibrational transition, rather than the electronic transition, is rate determining. This means that the crossing shown in Figure 3.5 actually would not occur and that the electronic states are mixed by the vibration in the region where the crossing occurs. This is usually the case for radiationless electronic transitions involving no change in spin. Such crossings for molecules are more complicated in polyatomic molecules and are discussed in Chapter 6.

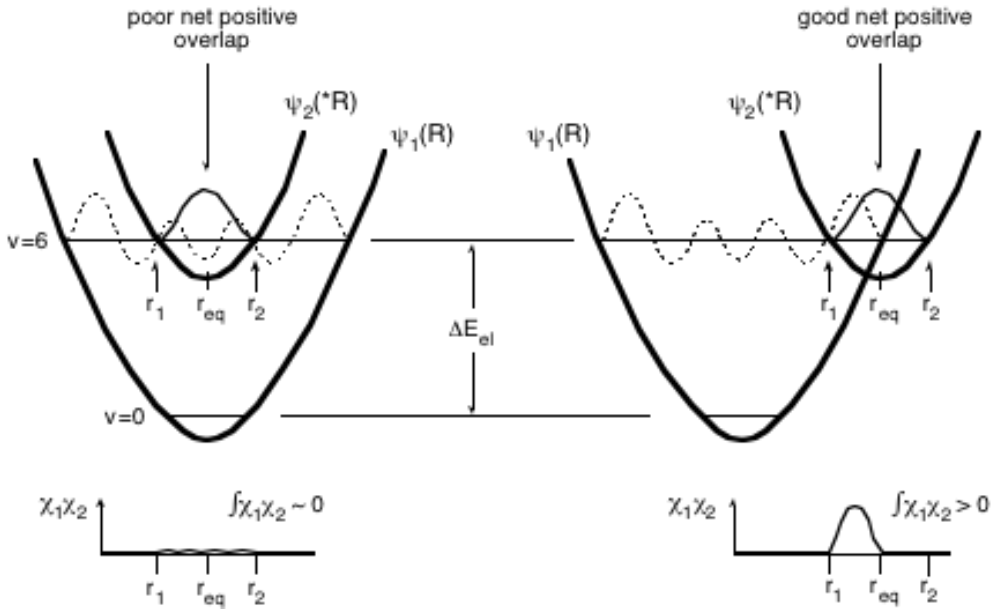

Figure 3.5. ***Schematic representation of situations for poor (left) and good (right) net positive overlap of vibrational wave functions. The value of the integral $\chi_i\chi_j$ as a function of r is shown at the bottom of the figure.***

3 .12 *Transitions between Spin States of Different Multiplicity. Intersystem Crossing*

We have developed a working paradigm for radiative and radiationless vibronic (electronic and vibrational) transitions between states of the same spin, based on the classical and quantum mechanical representation of the Franck-Condon principle. We now will develop a working paradigm for radiative and radiationless transitions involving a change of spin (change of spin multiplicity) employing the vector model for electron spin developed in Chapter 2. The spirit of the paradigm for spin transitions will be similar to that for electronic and vibronic transitions. As before, we postulate that for all transitions, energy and momentum must be conserved and transitions are "allowed" or "probable" only when the initial state and final state "look alike" in term of structure and motion. As we have seen, "looking alike" means that the initial and final states have electronic, vibrational and spin structures and associated motions and momenta that are similar. The basic concept is that abrupt changes in electronic, vibrational or spin structure and/or motion are inherently resisted by natural systems. The fastest transitions occur when two systems possess similar wavefunctions and energies. When this is the

case the wavefunctions are “in resonance” and interact strongly and the system oscillates rapidly between both states.

We will now develop a model of a precessing vector representing the spin wave function, **S,** that is analogous to the pictorial model developed for vibrating nuclei or orbiting electrons. We shall consider the spin wavefunction of an initial spin state, $\mathbf{S_1}$ and a final spin state, $\mathbf{S_2}$. Analogous to the electronic overlap integral $<\psi_1|\psi_2>$ and the vibrational overlap integral, $<\chi_1|\chi_2>$ there is a spin overlap integral $<\mathbf{S_1}|\mathbf{S_2}>$. When there is no spin change during the transition $<\mathbf{S_1}|\mathbf{S_2}> = 1$ (e.g., singlet-singlet, triplet-triplet, doublet-doublet), the initial and final states look alike in all respects and there is no spin prohibition on the electronic transition. However, when there is a spin change during the transition, $<\mathbf{S_1}|\mathbf{S_2}> \neq 0$ (e.g., singlet-triplet) and in the Zero Order approximation, the transition is strictly forbidden. In First Order transitions between singlets and triplets becomes allowed if a mechanism for mixing spin states is available. In contrast to the mixing of electronic states, the mixing of spin states requires ***magnetic interactions.***

A change in a spin state is termed ***intersystem crossing*** and corresponds to the reorientation of an electron spin vector or more formally to a transition involving a change in spin multiplicity, since different multiplicities correspond to different relative orientations of electron spins (Section 2.26). The most important intersystem crossings for organic photochemistry involved the interconversion of singlet states (S, multiplicity = 1) and triplet states (T, multiplicity = 3). Examples of intersystem crossing from Scheme 3.1 are $^*R(S_1) \rightarrow {}^*R(T_1)$ and $^3I(D) \rightarrow {}^1I(D)$.

Since there are three sublevels (T_+, T_0 and T_-) to every triplet state T, we need to consider the possible mechanisms of transitions of each of these states to the singlet, S, and the corresponding transitions of S to each of the triplet states. We also need to consider the possible magnetic interactions (e.g., spin-orbit interactions) that are available which can "mix" the singlet and triplet states so that they "look alike".

Intuitively, we might expect that there will be a paradigm analogous to the Franck-Condon principle for spin transitions. The Franck-Condon principle is based on the Zero Order assumption that the rates of electron orbital motions (typical rates 10^{15}-10^{16} s^{-1}) are much faster than nuclear motions (typical rates 10^{14}-10^{12} s^{-1}) so that during an electronic transition, the nuclei are "frozen". This assumption breaks down in first Order

when there is significant mixing of the vibrational and electron motion. Similarly, in Zero Order for intersystem crossing transitions, we assume that the rates of electron orbital motions are much faster than the rates of precessional motions of electron spins (quantitative justification of this assumption will be given below). Thus, the paradigm states that intersystem crossing between electronic states is generally improbable in Zero Order and we must seek mixing interactions that allow intersystem crossing to occur. Spin mixing mechanisms can result from interactions and couplings of the electron spin magnetic moment with other magnetic moments. For transitions between electronic states in organic molecules only ***spin-orbit coupling*** (Scetion 3.31) is generally of greatest importance for inducing spin transitions. However, for radical pairs and biradicals, we shall see that spin-orbit coupling, Zeeman coupling and spin-nuclear hyperfine coupling may all be capable of inducing intersystem crossing.

3.13 *Classical Precession of the Angular Momentum Vector*

In section 2.24 we developed a model representing the electron spin angular momentum, **S** as a vector. The latter possesses a magnetic moment, $\boldsymbol{\mu}$ that is associated with its electron spin (Eq. 2.32). In the absence of any other magnetic fields (other magnetic moments), both **S** and $\boldsymbol{\mu}$ vectors are imagined to lie motionless in space and to possess a single energy. The situation is quite different when there are any magnetic fields coupled with the magnetic moment of the spin. The result of such a coupling is that the electron spin and its associated magnetic moment will (1) either line up in a direction aligned with the coupling field or in a direction opposed to the coupling field and (2) depending on its orientation, make a clockwise or counterclockwise precessional motion about the axis of the magnetic field or the coupling field. Precession is defined as the motion of the axis swept by a spinning body, such as a gyroscope (Figure 3.6). From classical physics we know that the precession of the axis of a spinning body sweeps out a conical surface, and the tip of the precessing axis sweeps out a circle.

We now consider a model of this precessional motion for a classical bar magnet and then adapt the classical model to electron spin, a quantum mechanical magnet. The classical bar magnet in a magnetic field was employed as a simple physical model of the

energy states of a magnetic moment derived from an electron spin coupled to a magnetic field (Section 2.33). If the bar magnet in a magnetic field possessed angular momentum by spinning about an axis, it would execute a precessional motion about the axis defined by the applied magnetic field. A classical analogue of the expected motion of a magnet possessing angular momentum in a magnetic field is available from the precessional motion of a rotating or spinning body such as a toy top or a gyroscope (Figure 3.6). The angular momentum vector of a spinning top sweeps out a cone in space as it makes a **precessional** motion about the axis of rotation, and the tip of the vector sweeps out a circle (Fig. 3.6, left). The cone of precession of a spinning top possesses a geometric form identical to the cone of possible orientations that are possible for the quantum spin vector, so that the classical model can serve as a basis for understanding the quantum model.

A remarkable, and non-intuitive, feature of a spinning top is that it appears to defy gravity and precesses, whereas a non-spinning gyroscope falls down! The cause of the precessional motion and the top's stability toward falling is attributed to the operation of the force of gravity, which pulls downward, but exerts a torque "sideways" on the angular momentum vector. This torque produces the non-intuitive result of precession. ***By analogy, in the presence of an applied field, we imagine that the coupling of a spin's magnetic moment with the magnetic field produces a torque that, like gravity for the top, "grabs" the magnetic moment vector, μ, and causes it to precess about the field direction.*** Since the spin's magnetic moment and angular momentum vectors are collinear, the angular momentum vector, **S**, also precesses about the field direction (Fig. 3.6).

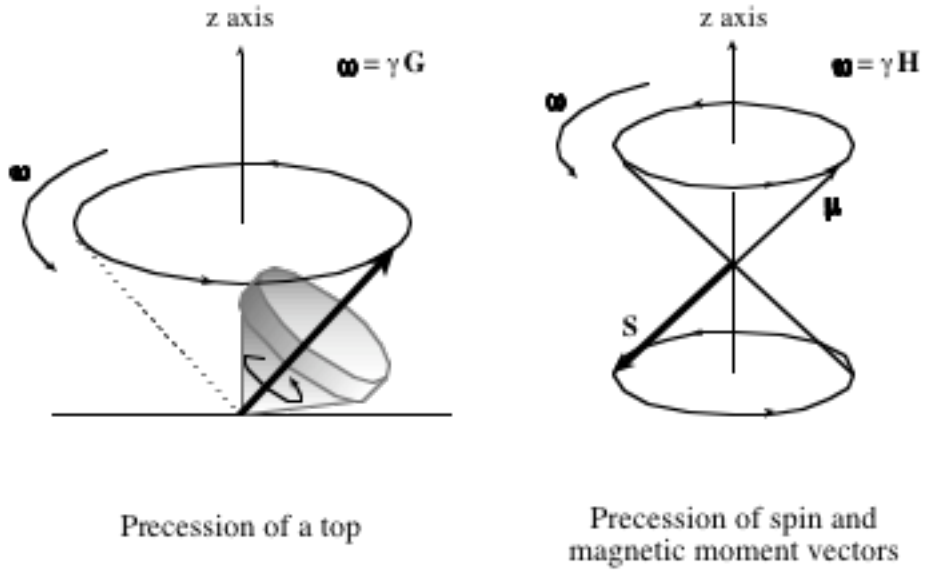

Figure 3.6. ***A vector diagram comparing the precessional motion of a spinning top to the precessional motion of spin angular momentum vector S and the precessional motion of the magnetic moment, μ_S in the presence of an applied magnetic field.***

The classical vectorial properties of the angular momentum of a toy top or gyroscope (Fig. 3.6, left) are analogous to many of the important characteristics of the vectorial properties of the quantum mechanical magnetic moment associated with electron spin. The reason for the close analogy is due to the important and ***critical connection between the electron's magnetic moment and the angular momentum due to the electron's spin***. For example, the rotating mass of a gyroscope possesses angular momentum that can be represented by a vector whose direction is along the symmetry axis of rotation. A gyroscope in a gravitational field precesses, i.e., the axis of its rotation rotates or precesses with an angular frequency ω about the direction of the gravitational field. The angular frequency ω is a vector quantity.

There are two factors determining the frequency, ω, of precession of a gyroscope: **the force of gravity (G) and the magnitude of spin angular momentum (S) of the spinning gyroscope**. If the spin angular momentum, **S**, which is determined by the angular velocity of spin and the mass of the gyroscope, is constant, then the rate of

precession $\boldsymbol{\omega}$ is determined only by the force of gravity, so that there is a proportionality between the rate of precession and the force of gravity, **G**, as shown in Eq. 3.10, where γ (compare to the magnetogyric ratio in Eq. 2.32) is a scalar proportionality constant between the precessional frequency and the force of gravity.

$\boldsymbol{\omega} = \gamma\mathbf{G}$ Precession in a gravitational field (3.10)

$\boldsymbol{\mu} = -g_e\gamma_e\mathbf{S}$ Precession in a magnetic field (2.32)

The mathematical form of the dynamics of the precessional motion of a gyroscope (Eq. 3.10) in the presence of gravity is the same as the mathematical form of the dynamics of a magnetic moment associated with precessional motion of a spinning charged body in the presence of a magnetic field (Eq. 2.31). We shall therefore postulate that the vector due to the magnetic moment of the quantum magnet, $\boldsymbol{\mu}$, undergoes precessional motion in an applied magnetic field and that the frequency, ω., of the precessional motion will have a mathematical for analogous to Eq. 3.10.

Let us consider the specific case for which the amount of spin angular momentum is equal to $\hbar$, the fundamental unit of angular momentum in the quantum world (i.e., the value of the angular momentum for a spin 1 system, i.e., $\mathbf{S} = 1$). In analogy to Eq. 3.10, for this case the spin angular momentum vector and the magnetic moment vector due to spin precess about the field direction with a characteristic angular frequency, ω, given by Eq. 3.11, where γ_e is the magnetogyric ratio of the electron and **H** is the (absolute value of the) strength of the magnetic field.

ω (Larmor frequency) $= \gamma_e|\mathbf{H}|$ (3.11)

For the special case corresponding to one unit of angular momentum, $\hbar$, the rate of precession, ω, of the spin and magnetic moment vectors about the magnetic field **H** **depends only on the magnitude of γ_e and H** . This special precessional frequency is termed the **Larmor** frequency and should be familiar to students who have studied NMR or EPR spectroscopy.

We noted in Chapter 2 that an important feature differentiating the classical magnet from the quantum magnet is that a classical magnet may assume any arbitrary position in an applied field (of course, the energy will be different for different positions), but the quantum magnet can only achieve a finite set of orientations defining a **cone of possible orientations** with respect to an axis defined by an arbitrary axis. When the spin takes on one of these allowed orientations, it is required to be somewhere in the cone of possible orientations, but does not precess. However, upon applications of a constant magnetic field that couples to the electron spin, we imagine that the field imposes a constant torque on the magnetic moment of the electron spin. The latter then immediately begins to precess about the magnetic field axis (we choose this axis for convenience since the selection of the quantization axis is arbitrary) and that this precessional motion sweeps out one of the cones of possible orientations (Section 2.29)**.**

Thus, we postulate that in the presence of a magnetic field, for each allowed orientation of the electron spin there exists a ***cone of possible precession for the angular momentum and magnetic moment vectors associated with the electron's spin and that the frequency of precession in these cones is proportional to the strength of the coupling magnetic field.*** This is a remarkable conclusion that has far reaching consequences in molecular organic photochemistry for processes involving a change of multiplicity.

3.14 *Precession of the Quantum Magnet in the Cones of Possible Orientations.*

We have now seen that the positions of individual spin vectors in mathematical vectorial space are confined to cones that are oriented along an arbritrary quantization axis. Furthermore, the **cones of possible orientations** (for each value of the spin orientation quantum number, M_S) of the angular momentum vector also represent **cones of precession** when the spin vector is subject to a torque from some coupling magnetic field. When a magnetic field is applied along the z axis, ***the spin states with different values of M_S will assume different orientations in the magnetic field and will possess different energies because of the different orientations of their magnetic moments in the field*** (recall from Eq. 2.32 that the direction of the magnetic moment vector is

collinear with that of the angular momentum, so if the angular momentum possesses different orientations, so will the magnetic moment). These different energies, in turn, correspond to different angular frequencies of precession, ω, about the cone of orientations. In analogy to Eq. 2.32, we can formulate Eq. 3.12 for the energy E_Z of a specific orientation of the angular momentum in a magnetic field is directly proportional to M_S, μ_e and $\mathbf{H}_Z$ (see Eq. 2.34, Chapter 2).

$$E_Z = \hbar\omega_S = M_S g\mu \mathbf{H}_Z \qquad (3.12)$$

From Eq. 3.12 the value of the spin vector precessional frequency, ω_S, is given by Eq. 3.13.

$$\omega_S = [M_S g\mu \mathbf{H}_Z]/\hbar \qquad (3.13)$$

From Eq. 3.13, the values of ω_S are directly related to the same factors as the magnetic energy associated with coupling to the field, namely, the amount of angular momentum along the axis, the magnetic moment and the magnetic field strength. For two states with the same absolute value of M_S, but different signs of M_S, the precessional rates, ω_S, are **identical in magnitude, but opposite in the sense (phase) of precession.** If the tips of the vectors in Fig. 3.6 were viewed from above, they either trace out a circle via a clockwise motion for the lower energy, M_S = -1 state and trace out a circle via a counterclockwise motion for the higher energy, M_S = +1 state. These senses of rotation correspond to differing orientations of the magnetic moment vector in a magnetic field and therefore different energies, E_Z.

From classical physics, the rate of precession of a magnetic moment about an axis is proportional to the strength of coupling of the magnetic momentum to that axis (in analogy to Eq. 3.11). The same ideas hold if the coupling is due to sources other than an applied field, i.e., coupling with other forms of angular momentum. For example, if coupling of the spin angular momentum, **S** with the orbital angular momentum, **L** (spin-orbit coupling) is strong, then the vectors **S** and **L** precess rapidly about their resultant and are strongly coupled. The idea is the same as the strong coupling of two electron spins (two doublets, D) of angular momentum 1/2, to form a new spin system, a triplet (T) of spin 1 or a singlet (S) of spin 0. When the coupling between the angular momenta is strong, the precessional motion about the resultant is fast and is difficult for other

magnetic torques to break up the resultant coupled motion. However, if the coupling is weak, the precession is slow about the coupling axis and the coupling can be broken up by relatively weak magnetic forces. These ideas will be of great importance, because they provide insight to the mechanism of **transitions involving a change of spin**, such as intersystem crossing, between magnetic states.

Since the magnetic moment vector and the spin vector are collinear (but opposite in direction, Figure 3.6, right), ***these two vectors will faithfully follow each other's precession, so that we do not need to draw each vector, since we can deduce from the characteristic motion of one vector the characteristic motion of the other.*** We must remember, however, that the angular momentum vector has the units of angular momentum ($\hbar$), and the magnetic moment vector has the units of magnetic moment (J/G). Figure 3.7 shows the vector model of the different types of precession for a spin 1/2 and spin 1 states in their possible cones of orientation.

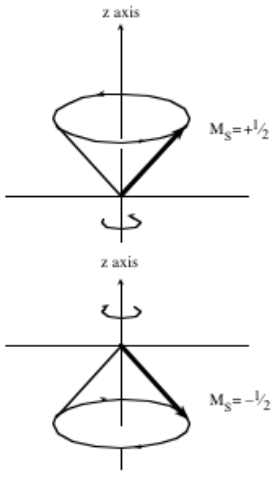

Precessing vectors representing the spin angular momentum of a spin $1/2$ particle in a magnetic field

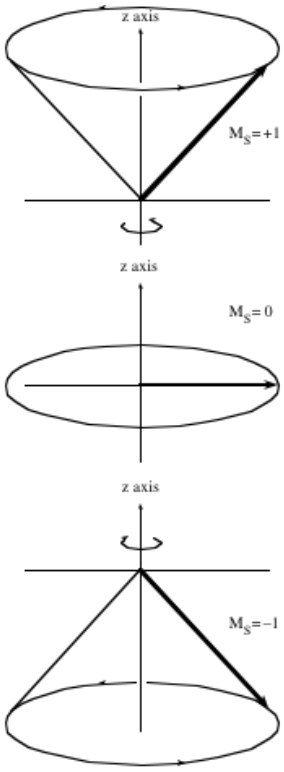

Precessing vectors representing the spin angular momentum of a spin 1 particle in a magnetic field

Figure 3.7. ***Vector model of vectors precessing in the possible cones of orientation. Only the spin angular momentum vectors are shown. The magnetic moment vectors (μ) (see Figure 3.6) precess at the same angular frequency as the angular momentum vectors (S), but are oriented collinear and 180^o with respect to the spin vector. The magnitude of the angular momentum vector for the S = 1 system (right) is twice the magnitude of the angular momentum vector of the S = 1/2 system (left).***

3.15 *Summary*

The process of rotation of the quantum magnet's vector about an axis such as that of an applied magnetic field is termed **precession,** and the specific precessional frequency of a given state under the influence of a specific field, $\mathbf{H_Z}$, is termed the **Larmor precessional frequency, ω_Z**. We note the following characteristics of the Larmor precession, all of which are deduced from Eq. 3.13:

(1) The value of the precessional frequency ω_Z is proportional to the magnitude of the four quantities M_S, g, μ and $\mathbf{H_Z}$, where $\mathbf{H_Z}$ is the value of a magnetic field interacting with the spin magnetic moment.

(2) For a given orientation and magnetic moment, the value of ω_Z decreases with decreasing field, and in the limit of $\mathbf{H_Z} = 0$, the model requires precession to cease and the vector to lie motionless at some indeterminate value on the cone of possible orientations.

(3) For a given field strength and for a state with several values of M_S (multiplicity 1 or greater than 1), the spin vector precesses fastest for the largest absolute values of M_S and is zero for states with $M_S = 0$ (e.g., T_0 and S).

(4) For the same absolute value of M_S different signs of M_S correspond to different directions of precession, which have identical rates, but different energies (e.g., T_+ and T_-).

(4) A high precessional rate ω_Z corresponds to a strong coupling to the field $\mathbf{H_Z}$ and the magnetic energy corresponds to the strength of the coupling field.

(5) For the same field strength and quantum state, M_S, the precessional rate is proportional to the value of the g factor and the inherent magnetic moment μ.

3.16 *Some Quantitative Relationships Between the Strength of a Coupled Magnetic Field and Larmor Frequency*

From Eq. 3.13 and the experimental value of γ_e (1.7×10^7 rad s^{-1}) a quantitative relationships can be obtained between the precessional frequency, ω, and the coupling to an arbitrary magnetic field, **H**, for a "free" electron (Eq. 3.14):

$\omega = 1.7 \times 10^7$ rad s^{-1} **H,** where **H** is in the units of Gauss (3.14)

We are familiar to the relationship of the energy of a photon or an energy gap to a frequency or oscillation of a light wave, ν (Eq. 1.1).

$\Delta E = h\nu$ (1.1)

The relationship between the precessional frequency ω (rad s^{-1}) and the oscillation frequency ν (s^{-1}) is $\nu = \omega/2\pi$ or $\omega = 2\pi\nu$. The latter relationships between ω and ν when applied to Eq. 3.14 lead to Eq. 3.15:

$\nu = 2.8 \times 10^6$ s^{-1} **H** (**H** in Gauss) (3.15)

Thus, for a coupling field of 1 G, the precession rate of an electron spin is 2.8×10^6 s^{-1} (2.8 MHz) or ca 17×10^6 rad s^{-1}. Since one complete cycle about a circle is equivalent to 2π radians, for a fixed field the value of ω is always a large number than the value of ν. Eq. 3.16 provides the relationship of the precessional frequency, ω, the resonance frequency of radiative transitions, ν and the energy gap between the states undergoing transitions, ΔE.

$\Delta E = h\nu = \hbar\omega$ (3.16)

We can now compute some values for precessional frequencies and compare the results to the values of the frequencies previously discussed for electronic motion in orbits and the vibration motion of bonds. From Eqs. 3.14 and 3.15, we can compute (Table 3.1). Practically speaking, applied laboratory fields whose strengths can be varied from 0 to about 100,000 G are readily achievable, so that precessional rates ω up to the order of 1.7×10^{11} rad s^{-1} ($\nu = 2.8 \times 10^9$ s^{-1}) are achievable by applying laboratory magnetic fields to a free electron spin. Internal magnetic fields resulting from interactions with other electron spins or nuclear spins typically correspond to magnetic fields in the range from a fraction of a G to several hundreds of G. In certain cases,

however, strong spin-orbit coupling interactions or strong coupling of two electron spins, can produce magnetic fields of the order of 1,000,000 G or larger, causing precessional frequencies of the order of 10^{12} s^{-1} (1.7×10^{13} rad s^{-1}) and greater.

Table 3.1. Relationship Between the Rate of Precession of an Electron Spin as a Function of Magnetic Field Strength.

H (Gauss)	ω (rad s^{-1})	ν (s^{-1})
1	1.7×10^{7}	2.8×10^{6}
10	1.7×10^{8}	2.8×10^{7}
100	1.7×10^{9}	2.8×10^{8}
1000	1.7×10^{10}	2.8×10^{9}
10000	1.7×10^{11}	2.8×10^{10}
100000	1.7×10^{12}	2.8×10^{11}
1000000	1.7×10^{13}	2.8×10^{12}

Now we can compare the range of frequencies for precessional motion to the rates of electronic orbital and nuclear vibrational motion. Since electronic and vibrational frequencies refer to "back and forth" linear periodic motion, whereas precessional motion refers to a circular periodic motion, we shall compare the rates of motion of the three systems in frequency units (s^{-1}). Electronic motions in orbitals are typically of the order of 10^{15}-10^{16} s^{-1} and vibrational motions of the functional groups or organic moleculess are typically of the order of 10^{12}-10^{14} s^{-1}. Electron spins in a very strong magnetic field of 1,000,000 G precess at a rate of only 10^{12} s^{-1} (Table 1) and precess at still slower than electronic and vibrational motion at weaker, more common magnetic fields. Thus, the assumption, in Zero order, that electronic and vibrational motions are much faster than spin motion is justified. We can now articulate a "Franck-Condon" rule for spin transition. During the time for an electronic transition or a vibration (10^{-12} s or less) the precessing spin is "frozen" in its precessional cone. Like all approximations this one is subject to breakdown in special situations (exceptionally strong spin-orbit coupling). However, for organic molecules this approximation holds well. We'll discuss the conditions for the breakdown of the approximation (e.g., the heavy atom effect for

inducing intersystem crossing) in Chapter 4. We now will consider some examples of magnetic coupling which are required for intersystem crossing to occur.

3.17 *Transitions between Spin States. Magnetic Interactions and Magnetic Couplings.*

Transitions between the spin magnetic energy levels can be visualized as occurring through the result of magnetic ***torques*** exerted on the magnetic moment vectors, $\boldsymbol{\mu}$, of an electron spin, or equivalently, as the result of coupling of spin angular momentum to another form of angular momentum, in particular, ***orbital*** angular momentum. Whether the magnetic coupling which causes the transition is spin-orbit, Zeeman or hyperfine, the same vector model allows the transitions resulting from the coupling of an electron spin to any magnetic moment to be visualized in an analogous form. These features of the vector model provide a powerful and general tool for visualizing intersystem crossing and for understanding electron spin resonance (and nuclear magnetic resonance) through a single common conceptual framework.

3.18 *The Role of Electron Exchange in Coupling Spins*

The exchange of electrons (Pauli Principle) is a non-classical quantum effect resulting in a splitting of singlet and triplet states (Section 2.10). The same electron exchange is also responsible for a coupling of the spin vectors, since upon exchange all properties of the electron must be preserved, including the phase of the relative orientations of the electron spin. When the exchange interaction, J, is strong between two spins, the latter are strongly coupled and must remain either in phase as a spin 1 system (triplet) or out of phase as a spin 0 system (singlet). The mathematical form of J in a spin Hamiltonian H_{ex} (the operator that indicates the interaction energies) is given by Eq. 3.17. The singlet triple splitting energy (ΔE_{ST}) is defined as 2J (a splitting of J above and below the energy corresponding to no exchange, Section 2.10).

$$H_{EX} = J\mathbf{S}_1 \cdot \mathbf{S}_2. \qquad (3.17)$$

Although the electron exchange is effectively a Coulombic (electrostatic) interaction and not a magnetic interaction per se, it influences magnetic couplings in two important ways: (1) the exchange interaction causes the singlet and triplet states to be different in energy, making it more difficult for them to couple magnetically because energy must be conserved during intersystem crossing; and (2) for the two electrons in a strong exchange situation the spins are tightly electrostatically coupled to each other because of the operation of the Pauli Principle, again making intersystem crossing difficult because a strong magnetic force must be applied to decouple the two spins. When the energy gap, J, is much larger than available magnetic energy, singlet-triplet interconversions are said to be "quenched" by the exchange interaction J. In this case we view the two spin vectors to be precessing about each other to produce a net spin 1 resultant, and it is no longer meaningful to think of the individual spins as two component 1/2 spins!

The magnitude of J depends on the "contact" or extent of orbital overlap of the electron spins (Section 2.12). This exchange energy as a function of overlap of electronic orbitals of the two spins orbitals is approximated as an exponential function of the separation of the two orbitals (e.g., Eq. 3.18, where J_0 is a parameter which depends on the orbitals and r is the separation of the orbitals in space).

$$J = J_0 \exp -r \qquad (3.18)$$

The exchange interaction plays an important role with respect to intersystem crossing, since it “couples” two electron spins through electron exchange. The stronger this coupling, the stronger the value of any competing magnetic field must be to uncouple the spin motion and the weaker the coupling the better the chance that a weak competing magnetic field will induce intersystem crossing.

3.19 *Couplings of a spin with a magnetic field. Visualization Intersystem Crossing*

From the vector model of the triplet state (Section 2.26), we now can deduce for processes such as $^*R(S_1) \rightarrow {}^*R(T_1)$ and $^3I(D) \rightarrow {}^1I(D)$, ***that there are three distinct intersystem crossing transitions possible from a S state***, depending on whether the final state is T_+, T_0 or T_-: $S \rightarrow T_+$; $S \rightarrow T_0$ or $S \rightarrow T_-$.

As an exemplar of how the vector model for electron spin provides a general visualization of intersystem crossing, let us consider the specific example of the intersystem crossing of a T_0 state to a degenerate S state or *vice-versa* (Figure 3.8, top) or the intersystem crossing of a T_+ state to a degenerate S state or *vice-versa* (Figure 3.8, bottom). On the left and right sides of Figure 3.8 the two spins, $\mathbf{S}_1$ and $\mathbf{S}_2$, are represented as "spin bonded" or "tightly" coupled to each other (by electron exchange, J) by showing their precessional cones precessing about a common point. Intersystem crossing in such situations is "quenched" because the value of J is relatively large compared to available magnetic interactions and the singlet and triplets states are split apart from one another by $\Delta E_{ST} = J$. For intersystem crossing to occur, the electron exchange coupling must decrease to a value that is comparable to that of magnetic torques present in the system and is capable of acting on at least one of the spin vectors, say $\mathbf{S}_2$. This decrease in coupling, which occurs when the electrons and their spins separate in space, is indicated in Fig. 3.8 by showing the precessional cones separated by a dotted line to represent a "weakening" of the exchange interaction. An important exemplar of this situation in molecular organic photochemistry occurs for the $^3I(D) \rightarrow {}^1I(D)$, which involves the separation in space of the two doublet centers in a radical pair or biradical. For the intersystem crossing $^3I(D) \rightarrow {}^1I(D)$ to occur, a coupling is required by interaction of a magnetic moment from a third magnetic force, μ_3 with the magnetic moment one of the two spins $\mathbf{S_1}$ or $\mathbf{S_2}$.

From the vector model for electron spin, we expect two distinct "mechanisms" for intersystem crossing: (1) the magnetic interaction may occur along the z axis causing a "rephasing" of the spin vector $\mathbf{S}_1$ relative to $\mathbf{S}_2$, but does not causing a reorientation (spin flip) of $\mathbf{S}_2$ ($T_0 \rightarrow S$, transition, Figure 3.8, top) and (2) the magnetic interaction may occur along the x or y axis causing a spatial reorientation of the $\mathbf{S}_2$ vector relative to the $\mathbf{S}_1$ vector, i.e., the interaction causes a "spin flip" ($T_+ \rightarrow S$. Figure 3.8, bottom). The $T_- \rightarrow S$ transition (not shown) can be readily visualized by starting with two coupled β spins (two down spins) and performing an operation analogous to that in Fig. 3.8 bottom. The student of NMR will recognize that these two intersystem crossing

mechanisms are the same as the longitudinal relaxation and the transverse relaxation of magnetic nuclei in a magnetic field.

What are the magnetic forces that are available to interact with the magnetic moments of **S1** and **S2**? Typical sources of the magnetic couplings are spin-orbit interactions, Zeeman interactions, electron spin-nuclear spin interaction as indicated in Fig. 3.8.

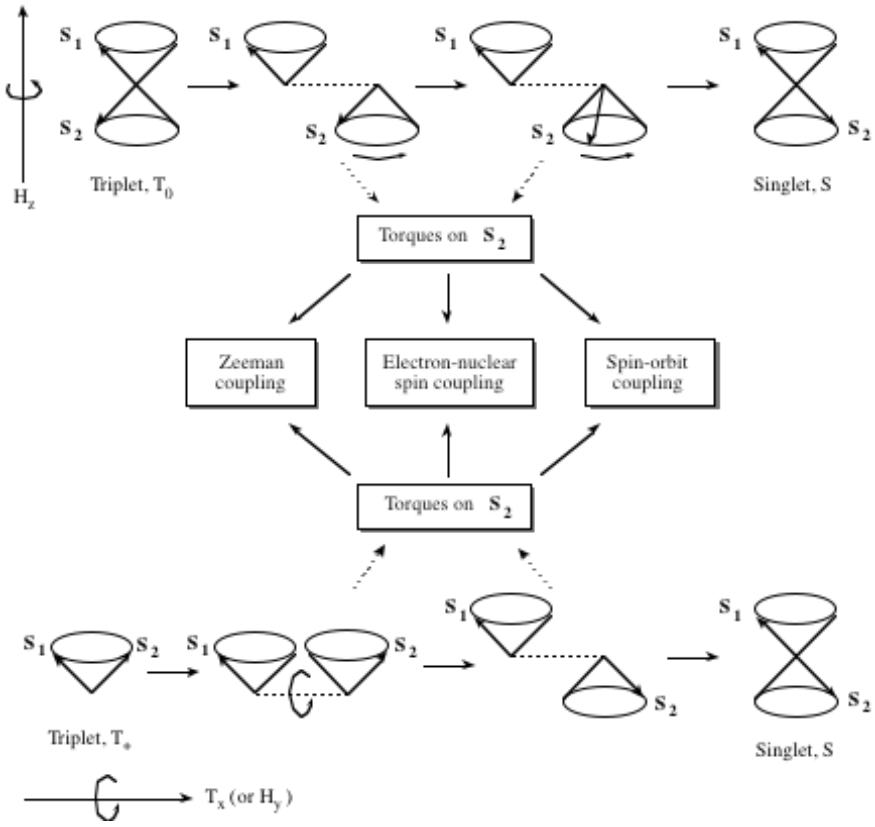

Figure 3.8. ***Example of magnetic couplings causing a triplet to singlet (or singlet to triplet transition. The torque on spin S_2 may result from the coupling of the magnetic moment of S_2 with magnetic moments due to any one of a numbers of sources as indicated in the figure.***

3.20 *Vector Model for Transitions between Magnetic States.*

A dominant selection rule for plausibility for electronic transitions in organic molecules is based on the conservation of spin angular momentum. The selection rule states that during an electronic transition, the electron spin must either remain unchanged or *change*

by one unit of angular momentum, ħ . The only way this selection rule can be obeyed when there is a spin change that is exactly compensated by an equal and opposite change of angular momentum of some sort. Any form of quantum angular momentum will do, not necessarily just electron spin angular momentum! For example, a photon possesses an angular momentum of 1 *ħ*, so it can couple to an electron spin and induce any of the plausible transitions between two spin states for which the spin changes by exactly one unit. This process for conservation of angular momentum is the basis of the rule that for radiative transitions the change in spin must be exactly 1 *ħ* (Chapter 4). As another example, a proton or a ^{13}C nucleus possesses a nuclear spin angular momentum **I** of 1/2 *ħ*, so hyperfine coupling with these nuclei can induce any of the plausible transitions if the change in the nuclear spin angular momentum (say +1/2 *ħ* → -1/2 *ħ*) is exactly the same as the change in the electron spin angular momentum **I** (say -1/2 *ħ* → +1/2 *ħ*) . As a final example, if an electron jumps from an s orbital ($l = 0$) to a p orbital ($l = \pm 1$) ,or *vice-versa*, the electron orbital angular momentum, **L,** changes by 1 *ħ*; if the orbital jump is coupled with a spin change of 1 *ħ* then spin orbit coupling can induce intersystem crossing.

3.21 *Spin-orbital Coupling. A Dominant Mechanism for Intersystem Crossing in Organic Molecules.*

Spin-orbit coupling is an important mechanism for "mixing" singlet and triplet states both in electronically excited states, *R and in diradical (or radical pair) intermediates I(D), Sch. 3.1. As usual, the selection rule for intersystem crossing can be expressed as the value of a matrix element. In this case, the matrix element for the coupling energy has the form $\langle\psi_1|H_{SO}|\psi_2\rangle$ where H_{SO} is the operator for spin-orbit coupling. Spin-orbit coupling is defined as the magnetic interaction between the magnetic moment due to the electron's spin angular momentum, **S**, with the magnetic moment due to the electron's orbital angular momentum, **L**. Physically, we can view spin-orbit coupling as the coupling of the magnetic moment due to electron spin to the magnetic

moment due to electron orbital motion. The strength of magnetic coupling depends on the orientation of the moments as well as their magnitudes (Section 2.39). The operator $\mathbf{H}_{SO}$ representing the energy of the spin-orbit coupling has the form of Eq. 3.19, where ζ_{SO} is termed the spin-orbit coupling constant and is related the nuclear charge that the electron sees as it orbits key atoms involved in the intersystem crossing. The magnitude of spin-orbit coupling, E_{SO}, will be given by a matrix element (Eq. 3.20).

$$\mathbf{H}_{SO} = \zeta_{SO}\mathbf{SL} \sim \zeta_{SO}\boldsymbol{\mu}_S\boldsymbol{\mu}_L \tag{3.19}$$

$$E_{SO} = \langle\psi_1|H_{SO}|\psi_2\rangle = \langle\psi_1|\zeta_{SO}\mathbf{SL}|\psi_2\rangle \sim \langle\psi_1|\zeta_{SO}\boldsymbol{\mu}_S\boldsymbol{\mu}_L|\psi_2\rangle \tag{3.20}$$

The energy arising from the coupling is the vector product of the spin ($\boldsymbol{\mu}_S$) and orbital ($\boldsymbol{\mu}_L$) magnetic moments. In addition, because the matrix element (Eq. 3.1, $\mathbf{P} = \mathbf{H}_{SO}$) for spin-orbit interaction involves two electronic wavefunctions, ψ_1 and ψ_2, the magnitude of the matrix element also depends on the net (mathematical) overlap of the wavefunctions. We can now ask how the spin-orbit operator, H_{SO}, influences the overlap integral of the electronic wavefunctions, $\langle\psi_1|\psi_2\rangle$. The operator, $\mathbf{H}_{SO}$, is unusual compared to other operators we have encountered and requires some discussion and examination. As discussed earlier in Section 3.13, the visualization of the torques that operate when angular momentum is exchanged between systems is not intuitive. The non-intuitive nature of $\mathbf{H}_{SO}$ reflects the non-intuitive features of angular momentum discussed above for a gyroscope. Mathematically, $\mathbf{H}_{SO}$ "rotates" the orbital upon which it operates by 90°.

Let us select a specific, simple physical exemplar of a single electron atom (of nuclear charge Z) to understand how H_{SO} operates on ***atomic*** wavefunctions and how this operation has a major impact on the strength of spin-orbit coupling. Let's examine the spin-orbit coupling associated with an electron in a p-orbital, which is an important atomic orbital in forming n, π, and π* orbitals in excited molecules (*R) and radicals (I). An electron in a p-orbital possesses exactly one unit of orbital angular momentum, **L**, exactly the same amount of angular momentum required to change an electrons' spin orientation from α(+1/2) to β(–1/2) or from β(–1/2) to α(+1/2). However***, for angular***

momentum to be conserved during a change in spin orientation on a unit of angular momentum, the p-orbital which is coupled to the electron spin must change its orientation by exactly one unit of angular momentum. The p-orbital can do this by "rotating" about an arbitrary z-axis of rotation by 90^0, which is equivalent to rotating into an adjacent p-orbital (Fig. 3.9). It is this requirement to rotate about an axis in order to conserve angular momentum that is reflected in the form of the operator H_{SO}.

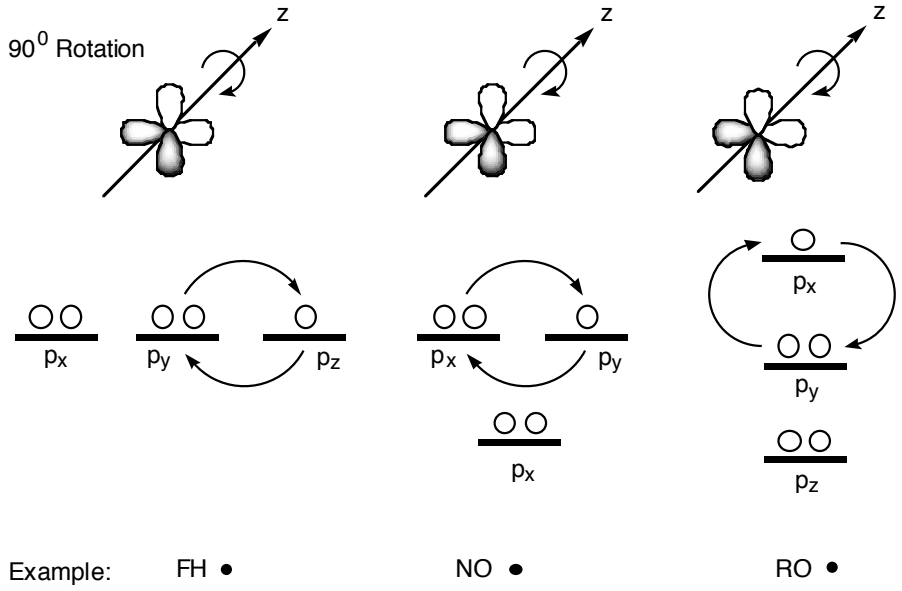

Figure 3.9. ***Schematic description of the effect of H_{SO} on the orientation of a p-orbital. H_{SO} "twists" a p-orbital 90^0.***

Let's now visualize the influence of H_{SO} on a p-orbital for two orbital situations shown in Fig. 3.9. Situation (a) corresponds to that for an atom which has spherical symmetry and for which all three p-orbitals are energetically degenerate (have exactly the same energy); situation (b) corresponds to that for a diatomic molecule which has cylindrical symmetry and for which two of the orbitals (in the x,y plane) are degenerate and have a different energy from the p orbital along the z-axis (usually involved in bonding and therefore somewhat lower in energy); situation (c) corresponds to a more general case for molecules which do not have a high degree of symmetry and for which all three atomic p orbitals have different energies.

For situations (a) and (b) the $p_x \rightarrow p_y$ jump occurs between orbitals of the same energy, but for situation (c) the $p_x \rightarrow p_y$ jump occurs between orbitals of different

energies. As we have seen many times, mixing of states with similar energies is much stronger than mixing of states with different energies. In this case ($p_x \rightarrow p_y$ jump) the mixing corresponds to the generation of *orbital angular momentum* which is needed to couple with the spin angular momentum. From Fig. 3.9 we can visualize the orbital motion "twisting" about an axis, which is the essence of generation of angular momentum. The larger the orbital angular momentum generated, the stronger the spin-orbit coupling. Thus, the closer the system is to case (a) or (b) in Figure 3.9, the stronger the spin-orbit coupling is, the faster the rate of intersystem crossing is, all other factors being similar.

Now instead of appealing to the angular momentum interactions, let consider the magnetic interactions which occur when the p-orbital rotates about the z-axis for case (a). The rotation corresponds physically to the "jump" of an electron from a p_x to a p_y orbital (the p_z orbital is oriented parallel or along the the z-axis) and it generates one unit of angular momentum about the z-axis. This orbital angular momentum possess an associated (Eq. 2.31) magnetic moment, $\boldsymbol{\mu}_L$, that couples with the spin's magnetic moment, $\boldsymbol{\mu}_S$, and induces spin reorientation or spin rephasing (Figure 3.8). The coupling of the spin and orbit magnetic moments means that the spin magnetic moment $\boldsymbol{\mu}_S$ serves as a torque which tends to twist the p-orbital and make it rotate 90^0 around the z-axis of rotation, and reciprocally, the orbital magnetic moment $\boldsymbol{\mu}_L$ serves as a torque which tends to twist the spin vector from an α to a β or from a β to an α orientation.

The matrix element $\langle\psi_1|H_{SO}|\psi_2\rangle$ is a measure of the magnitude (energy) of spin-orbit coupling. A remarkable feature of the operator H_{SO} is that it makes ψ_1 "look like" ψ_2 by mathematically *rotating* the wavefunction by 90^0! Let us attempt to visualize the effect of H_{SO} on the transition of a p_x to a p_z orbital, i.e, let us visualize the matrix element $\langle p_y|H_{SO}|p_x\rangle$. Since the mathematical operation of H_{SO} on p_x (the $H_{SO}|p_y$ part of the matrix element) is to rotate the p_x orbital by 90^0, the mathematical operation converts the p_x orbital into the p_y orbital.

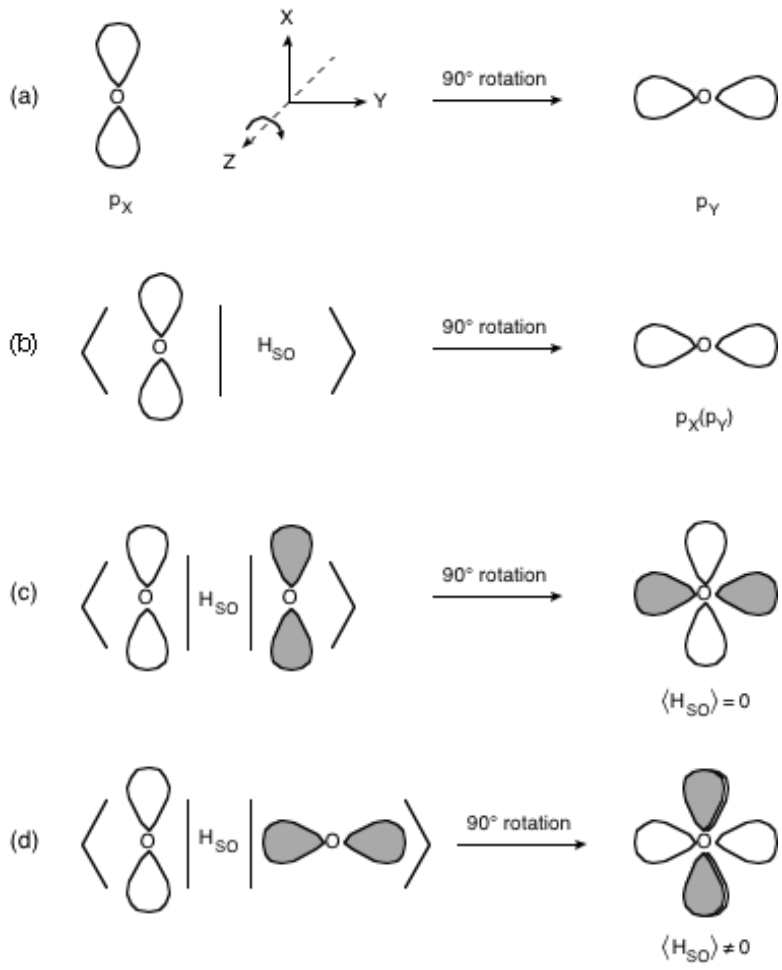

Figure 3.10. ***Visualization of the matrix element for spin-orbit coupling. See text for discussion.***

Now let's visualize the matrix element $<p_y|H_{SO}|p_x>$ and note that the extent of spin-orbit interaction will depend on the net mathematical overlap of the orbitals when the integral is computed, i.e., we seek to estimate the magnitude of the overlap integral which results after the mathematical operation $< H_{SO}|p_x>$ is performed. The mathematical operation $<H_{SO}|p_x>$ is visualized in Figure 3.10 a. The visualization of the electronic version of the operation $<H_{SO}|p_x>$ is shown in Fig. 3.10 b. If orbitals of the same type, say two p_x orbitals, are involved in the intersystem crossing the operation of H_{SO} on the p_x orbital converts it into a p_x orbital (Fig. 3.10 c). As a result of the operation $<H_{SO}|p_x>$ the overlap of a p_x with a p_y orbital is exactly zero, so the magnitude of the spin-orbit coupling matrix element $<p_x|H_{SO}|p_x>$ is exactly zero! On the other hand, let's now

imagine what happens when a p_x and p_y orbital are involved in the coupling (Fig. 3.10 d). In this case the operation of H_{SO} on p_y rotates the orbital 90^0 and converts it into a p_x orbital. Now the two orbitals involved in the interaction look exactly alike (Fig. 3.10d! Thus, for the matrix element $<p_x|H_{SO}|p_y>$ there is a good overlap integral and strong spin-orbit coupling. This aspect of H_{SO} corresponds to the operator selecting and connecting the correct orbital symmetries of transitions for generating maximum orbital angular momentum. This generates the maximal magnetic moment $\boldsymbol{\mu}$, since the magnitude of the **L** is proportional to $\boldsymbol{\mu}$ (Eq. 2.28).

The orbital motion of an electron in an organic molecule is much more complicated than that of an electron in a Bohr atom, which is assumed to be in a circular orbit moving at a constant velocity. Indeed, for electrons in molecules, a more realistic view is to consider the electron as moving in an orbital in which the electron moves in space about a framework of positively charged nuclei. For the case of an electron bound mainly to a single nucleus of charge Z, the electron spends some time relatively close to and some time relatively far away from the nucleus. According to relativistic quantum mechanics, when the electron approaches a nucleus, it accelerates to very high speeds because of electrostatic attraction to nucleus. The higher the nuclear charge Z, the greater the acceleration of the electron as it approaches the nucleus. Indeed, the speed of the electron must approach relativistic velocities in order to be "sucked" into the nucleus (on very rare occasions, the electron is captured by the nucleus, the inverse of β-nuclear decay!). The magnetic field generated by a moving charge is proportional to its velocity. Thus, when the electron is moving in the vicinity of the nucleus at relativistic velocities, its associated orbital magnetic moment, $\boldsymbol{\mu}_L$, may be huge. It is therefore expected that the coupling of the spin ($\boldsymbol{\mu}_S$) and orbital ($\boldsymbol{\mu}_L$) magnetic moments will be maximal when the electron is accelerating near the nucleus of charge Z. The larger the charge Z on the nucleus, the larger the acceleration the electron must achieve to avoid being sucked in to the nucleus. As a result, we expect a "heavy atom" effect (really a nuclear charge effect, Z) on the rate of spin-orbit induced transitions, i.e., as the nuclear charge Z increases, the degree of spin-orbit coupling increases, if the electron is in an orbital that allows a close approach to the nucleus to occur. The strength or energy, E_{SO}, of spin-orbit coupling is proportional to the spin-orbit proportionality constant ζ_{SO} of Eqs. 3.19 and 3.20.

From this primitive but useful pictorial model of spin-orbit coupling, the following generalizations can be made:

1. The strength or energy (E_{SO}) of spin-orbit coupling is directly proportional to the magnitude of the magnetic moment due to electron orbital motion, μ_L and the electron spin, μ_S.
2. The magnitude of E_{SO} will increase, for a given orbit, as Z, the charge on the nucleus increases, since the accelerating force attracting the electron is proportional and the spin-orbit coupling constant ζ_{SO} are proportional to Z (in an atom the proportionality is Z^n, where $n > 1$).
3. For maximum effect of the nuclear charge, the electron must be in an orbit that approaches the nucleus closely, i.e., an orbital with s-character.
4. Irrespective of the magnitude of E_{SO} for spin-orbit coupling to induce intersystem crossing, the total angular momentum of the system, orbit plus spin, must be conserved. For example, a transition from an α spin orientation to a β spin orientation (angular momentum change of one unit) may be completely compensated by a transition from a p-orbital of orbital angular momentum of 1 to a p-orbital of angular momentum 0 (e.g., a $p_x \rightarrow p_y$ transition).

These generalizations lead to the following selection rules for ***effective*** spin orbit coupling induced intersystem crossing in organic molecules:

Rule 1: The energy of the orbitals involved in the $p_x \rightarrow p_y$ transition must similar in energy (Figure 3.9).

Rule 2: Spin-orbit coupling in organic molecules will be effective in inducing intersystem crossing if a "$p_x \rightarrow p_y$" orbital transition on a single atom is involved in the transition between electronic states involved in the intersystem crossing, because this orbital transition provides both a means of conserving total angular momentum during the transition and also provides a means of generating orbital angular momentum that can be employed in spin-orbit coupling (Fig. 3.10).

Rule 3: Spin-orbit coupling in organic molecules will be effective in inducing intersystem crossing if one (or both) of the electrons involved approaches a "heavy" atom nucleus that is capable of causing the electron to accelerate and thereby create a strong magnetic moment as the result of its orbital motion (Eq. 3.20, $\zeta_{SO} \sim Z^n$, $n > 1$).

3.22 *Vector Representation of the Coupling of a Single Spin to Another Source of Angular Momentum*

Let us consider the simple case of a magnetic coupling of a single electron spin, $\mathbf{S_1}$ with some other, unspecified magnetic moment $\mathbf{H_i}$ from some arbitrary source. The latter is a vector quantity and therefore can be viewed as coupling effectively with $\mathbf{S_1}$ under the proper conditions. What are the proper conditions? They are identical for all effective magnetic couplings: (1) the magnetic moment of $\mathbf{S_1}$ must have a finite coupling or interaction with the magnetic moment $\mathbf{H}_i$; (2) the coupling is most effective when the two vectors possess identical Larmor frequencies and phases; (3) the strength of the magnetic coupling between $\mathbf{S_1}$ and $\mathbf{H_i}$ must be greater than the coupling of $\mathbf{S_1}$ to other magnetic moments.

Figure 3.11 provides a visualization of the coupling of a $\mathbf{S_1}$ to a second magnetic moment, $\mathbf{H_i}$. In the example, the spin function of $\mathbf{S_1}$ (shown as a solid vector) is taken to be α and the orientation of the angular momentum $\mathbf{H_i}$ (shown as an open vector) relative to the z-axis is arbitrarily taken to be opposite to that of $\mathbf{S_1}$. Since the source of $\mathbf{H_i}$ is not specified, it need not be an electron or nuclear spin and therefore strictly speaking, we should not use the terms α or β (which is reserved for spin functions) to describe $\mathbf{H_i}$ for the general case. However, for simplicity we shall assume that has exactly the same amount of angular momentum as that associated with the source of $\mathbf{H_i}$ and we shall use the terms α and β to signify the orientation of the angular momentum along the z-axis, since the concrete example of coupled spins follows exactly the same principles as any other magnetic coupling $\mathbf{H_i}$.

Returning to Figure 3.11a, we start the analysis by imagining that $\mathbf{S_1}$ and $\mathbf{H_i}$ are positioned in their cones of precession about the z-axis (Fig. 3.11a, left), but that the two spins are initially uncoupled and not interacting (dotted line separates cones). We then allow the coupling of the two vectors to occur (cones converge on z-axis). This coupling generates a resultant as shown in Fig. 3.11a, middle. If $\mathbf{H_i}$ were a spin 1/2 particle,

coupling of $\mathbf{S_1}$ and $\mathbf{H_i}$ could produce a final angular momentum state of 0 (singlet, S) or 1 (triplet, T). The triplet coupling would produce a T_0 state. We now imagine that the magnetic coupling between $\mathbf{S_1}$ and $\mathbf{H_i}$ is stronger than that of any other source of magnetic coupling available to $\mathbf{S_1}$. The result of this strong coupling causes the precession of the $\mathbf{S_1}$ and $\mathbf{H_i}$ about their resultant (Figure 3.11a, right). This precessional motion causes $\mathbf{S_1}$ to "flip" or oscillate periodically (Figure 3.11b) between the α and β orientations which we term $\mathbf{S_1}^{\alpha}$ and $\mathbf{S_1}^{\beta}$. This spin flip corresponds to the application of a magnetic field along the x or y axis. The situation in Fig. 3.11 b can be contrasted with that in Fig. 3.11c which shows both moments in the same cone of precession. In this case both magnetic moments precess about the z-axis at a rate determined by the larger of the two couplings: the two magnetic moment so each other or each to the field along the z-axis.

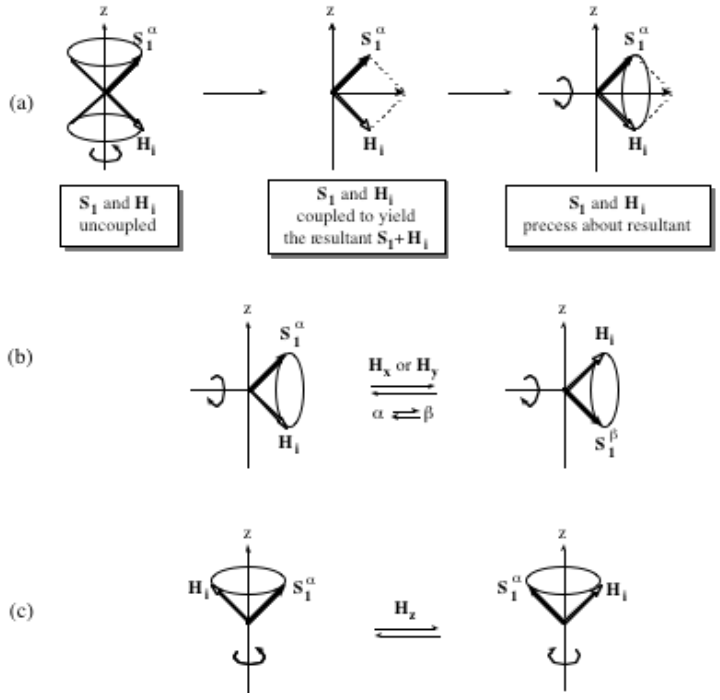

Figure 3.11. ***Vector representation of transitions of a single coupled electron spin, S_1. See text for discussion.***

In a radiative process involving the change in spin orientation, magnetic energy is conserved by coupling the magnetic moment of the spin with the oscillating magnetic moment of the electromagnetic field which possesses the correct frequency and phase for

the transition. In detail magnetic energy is conserved precisely by the energy of the absorbed or emitted photon, i.e., $\Delta E = h\nu$, where ν is the frequency required to achieve resonance and ΔE is the energy gap between the energy levels. Radiative transitions induced between magnetic sublevels (T_+, T_0 and T_-) are the basis of the field known as electron paramagnetic resonance spectroscopy (EPR) of paramagnetic doublet and triplet states (to be discussed in Chapter 4 and 8).

In the case of radiationless transitions between spin states, if the states undergoing transition are not exactly degenerate, then the magnetic energy gap between the two states undergoing the transition must be conserved by coupling with a "third" source of magnetic energy. The larger the energy gap between the two states undergoing the spin reorientation, the more difficult effective coupling becomes, and the transition becomes implausible or very slow. The energy conserving process for the radiationless transition may be accomplished by coupling the transition to the oscillating magnetic field produced by the motion of the components of the environment such as the molecules of a solvent (which possess magnetic moments due to nuclear spins and due to oscillating electric fields due to dispersion forces). This energy conserving process is viewed as a magnetic energy transfer between the spin system undergoing transition and some magnetic moments that are oscillating at the correct frequency in the solvent (the oscillating magnetic species in the solvent environment are termed the "lattice").

To maintain energy conservation, the lattice may either provide or absorb energy and can therefore assist in both spin jumps to higher energy and lower energy orbitals. With this description for the lattice we can imagine that the oscillating magnetic moments behave just like the oscillating magnetic field of electromagnetic radiation. Instead of photons, the lattice provides "phonons" or quanta of magnetic energy to the spin system. The lattice thus behaves analogously to a lamp emitting magnetic phonons or an absorber of magnetic phonons. The overall process is termed ***spin-lattice magnetic relaxation*** and is simply magnetic energy transfer between spin states. The most important interaction which couples the electron spin to the lattice is usually a dipolar magnetic interaction (Section 2.29, Eq. 2.33).

3.23 *Coupling Involving Two Correlated Spins. $T_+ \rightarrow S$ and $T_- \rightarrow S$ Transitions.*

The visualization of a single spin $\mathbf{S_1}$ coupled to a second spin, $\mathbf{S_2}$, (or any other generalized magnetic moment, $\mathbf{H_i}$) is a natural extension of the ideas of Fig. 3.11 and is shown in Figure 3.12 for two correlated spins (a singlet, S, or triplet, T, state) coupled to a third spin (or any other generalized magnetic moment, $\mathbf{H_i}$). Fig. 3.12 provides a vector model visualization of the important case of singlet-triple t and triplet-singlet intersystem crossing. In Figure 3.12 a, two electron spins, $\mathbf{S_1}$ and $\mathbf{S_2}$ in a T_+ ($\alpha\alpha$) state are shown as coupled to $\mathbf{H_i}$ (the coupling is indicated by showing the resultant vector produced by coupling and precession about the resultant). Now we suppose that a third spin, either an electron spin or a nuclear spin (represented as $\mathbf{H_i}$ in Fig. 3.12) is capable of coupling specifically to the spin $\mathbf{S_2}$ (Fig. 3.12 a, middle) in terms of a new resultant (thin arrow) which is followed by precession about the resultant), Fig. 3.12a, right. As was the case for the single coupled spin in Figure 3.11, the coupling of $\mathbf{S_2}$ to $\mathbf{H_i}$ causes $\mathbf{S_2}$ to precess about the x or y axis and to flip back and forth between the α and β orientations (Figure 3.12 b). From the vector diagram it is readily seen that this oscillation produced by coupling of $\mathbf{S_2}$ and $\mathbf{H_i}$ causes triplet (T_+) to singlet (S) intersystem crossing to occur in an oscillating manner as shown schematically in Fig. 3.12b.

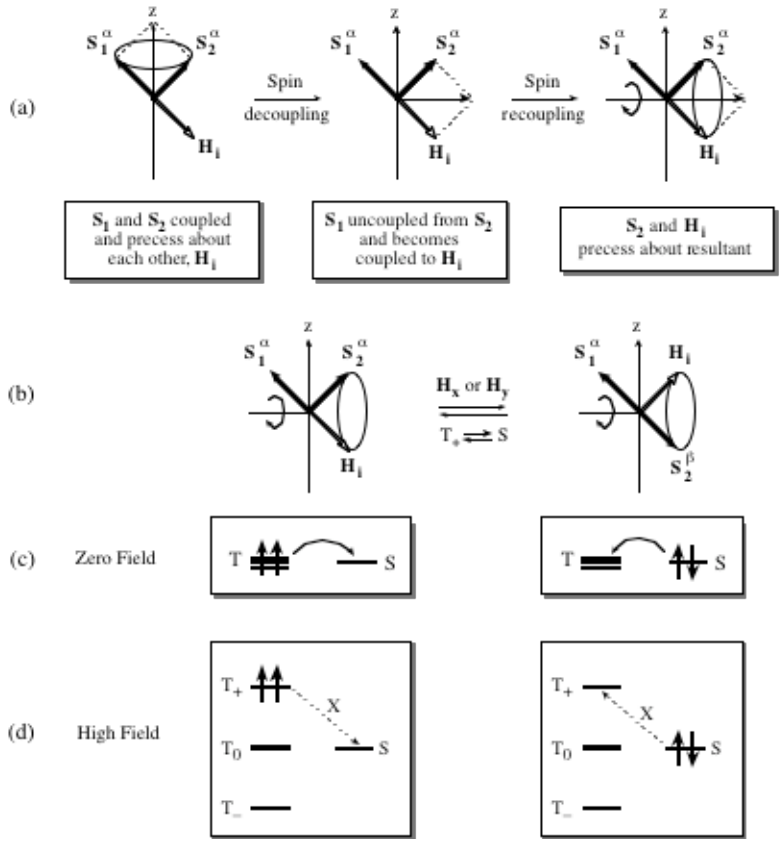

Figure 3.12. ***Schematic of two coupled spins coupled to a third spin. See text for discussion.***

At zero field (Fig. 3.12c) the singlet state (S) and the three triplet sublevels (T) are degenerate. Figure 3.12 c shows the situation for J = 0 at zero field ($\mathbf{H}_Z = 0$), and Fig. 3.12 d shows the situation for J = 0 at high field. There can be no radiative transitions between T and S possible at zero field because there is no energy gap between the states, and because an energy gap is required for a radiative transition, i.e., if a photon is absorbed there must be a source to accept its energy if energy is to be conserved.

At high field the $T_+ \rightarrow S$ (and $T_- \rightarrow S$) intersystem crossing (ISC) transitions are not plausible by radiationless pathways, because these transitions requires some source of magnetic energy conservation by coupling with the lattice. The plausibility of a radiative $T_+ \rightarrow S$ (and $T_- \rightarrow S$) ISC transition depends on the relative coupling of the electron spins to one another (i.e., on the value of J) and to the radiative field. If the

value of J is very small, the individual spins behave more or less independently so that radiative transitions of each spin ("doublet" transitions) become plausible. The vector diagram for the $T_- \rightarrow S$ transition is readily constructed from the symmetry relationships of the T_- vector representation to that of the T_+ vector representation. The conclusion from Fig. 3.12c and Fig. 3.12d is that when J = 0 and $\mathbf{H_Z} = 0$, ISC is plausible between all three triplet sublevels and of each of the three triplet sublevels and S, but that at high field only ISC between T_0 and S (or S and T_0) is plausible.

3.24 *Coupling Involving Two Correlated Spins. $T_0 \rightarrow S$ Transitions*

It is also possible for $\mathbf{H_i}$ to operate on a coupled electron spins along the z axis and to cause an ISC. However this situation is distinctly different from that shown in Fig. 3.12. As an exemplar, consider starting from an initial T_0 state ($\mathbf{S_1} = \alpha$ and $\mathbf{S_2} = \beta$, Fig. 3.13a). Under the conditions that J = 0, rephasing along the z-axis occurs if $\mathbf{H_i}$ is coupled selectively to one of the electron spins (say, $\mathbf{S_1}$). This rephasing causes $T_0 \rightarrow S$ ISC at **both** low field or at high field if J = 0.

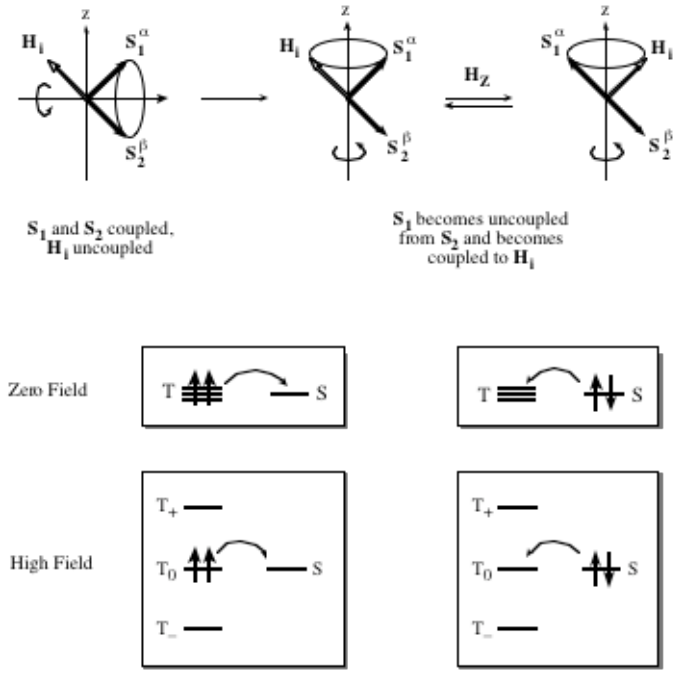

Figure 3.13. ***Vector representation of two correlated spins in a T_0 state coupled to a third spin along the z axis. See text for discussion.***

3.25 Summary

The transitions between two electronic states require the molecular wavefunctions corresponding to the initial and final states to look alike at the instant of transition. This corresponds to a resonance of the initial and final wavefunctions. The resonance is achieved only if energy and momentum are strictly conserved during the transition. If the conservation laws are obeyed, transitions may be induced by perturbations of the molecular wavefunctions through some appropriate coupling interaction such as electron-electron interactions, through electron-vibration induced transitions between different vibrational levels and through spin-orbit coupling. The Franck-Condon principle determines the relative probability of radiative and radiationless transitions between electronic states. As a consequence of the principle, the most probable radiative transitions occur "vertically" between electronic states of identical nuclear configuration, and radiationless transitions occur near crossings of potential energy curves. Intersystem crossing is most probable for organic molecules when the transition involves a p_x to p_y of comparable energy and capable of undergoing a transition on a single atomic center.

3.26 *The Effect of Electron Exchange on Intersystem Crossing*

Electron exchange, characterized by a coupling energy, J, between two electrons is an electrostatic and not a magnetic interaction. As a result one would not expect J to have a direct impact on the rate of triplet to singlet interconversions, which involve magnetic couplings. However, the magnitude of J does have an important impact on intersystem crossing because, as we have seen in the previous section, in order for a T→ S or S → T ISC to occur, the energies of T and S levels must be exactly equal to one another (degenerate) in order to conserve magnetic energy during the transition. Suppose that J = 0 and that he energies of the T and S states are equal in the absence of a magnetic field. This is the optimal situation for intersystem crossing since the energies of the S and T states are the same. However, even if J = 0, in the presence of a strong field, the T_+ and T_- states are knocked out or resonance (Fig. 3.12) with the S state by the

coupling of the T_+ and T_- states to the applied magnetic field. On the other hand, the coupling of the T_0 and S states persists if J = 0 (Fig. 3.12).

If $J \neq 0$, the entire triplet manifold of the T_+, T_- and T_0 states are knocked out of resonance with S (Fig. 2.15). This means that ISC becomes implausible and very slow. These effects of magnetic fields and J on ISC are very important for I(D) reactive intermediates as we shall see in Chapter 8.